NASA Contractor Report 195298

Design Considerations for a Space Station Radiation Shield for Protection from Both Man-Made and Natural Sources

Wesley E. Bolch, K. Lee Peddicord, Harry Felsher, and Simon Smith
Texas A & M University
College Station, Texas

December 1994

Prepared for
Lewis Research Center
Under Grant NAG 3-944

ACKNOWLEDGEMENTS

The authors would like to gratefully acknowledge the assistance and guidance of several individuals at NASA's Lewis Research Center (LeRC) and Johnson Space Center (JSC). In particular, the authors would like to thank Steve M. Stevenson (LeRC), the Project Manager for this study, and Alan J. Willoughby of the Analex Corporation, Cleveland, Ohio. This work was supported by the Advanced Space Analysis Office, NASA Lewis Research Center, under Grant NAG 3-944 with the Texas Engineering Experiment Station, Texas A&M University.

TABLE OF CONTENTS

Appendices

CHAPTER 1

INTRODUCTION

Over the past few years, mission planners within the National Aeronautics and Space Administration (NASA) have been considering various options for both power and propulsion in the initial design stages of NASA's Space Exploration Initiative or SEI. Nuclear power has played a key role in both these areas. For example, Nuclear Thermal Rocket (NTR) or Nuclear Electric Propulsion (NEP) systems have been examined extensively for both manned and unmanned missions to Mars. Current strategies also assume in-orbit construction of these vehicles possibly using an evolutionary version of NASA's space station (SS) or similar platform as a transportation node.

Texas A&M University has been working with NASA to examine operational scenarios involving the use of nuclear power and propulsion systems in the vicinity of NASA's space station. This work has focused on quantifying the radiological impact of these systems such that the integral radiation dose to the SS crew from both natural and man-made sources did not exceed allowable dose limits. Several of the scenarios developed relate to the use of SS as an evolutionary transportation node for lunar and Mars missions. The use of nuclear power on co-orbiting platforms and the storage and handling issues associated with radioisotopic power systems was also explored as they relate to SS.

In an earlier study (Bolch et al. 1990), four classes of scenarios were constructed and assessed. These included (1) the launch of both a typical NEP and NTR vehicle from low earth orbit (LEO), (2) the return of these vehicles to LEO, (3) the operation of a co-orbiting water electrolysis platform co-orbiting with SS, and (4) the storage and handling of radioisotope thermoelectric generators at the station. In each case, cumulative radiation doses were calculated and then compared to radiation dose budgets defined as the difference between the dose limit to the crew member and the dose contribution from natural space radiations in LEO. Key issues were identified to enable their proper incorporation into planning activities and to assess their proper impact upon baseline space station designs.

There are three fundamental options for reducing exposures to reactor radiation sources: time, distance, and shielding. By design, the earlier report by Bolch et al. (1990) investigated only the use of time and distance to reduce SS crew exposures to in-orbit

nuclear operations. In particular, the study focused on questions of reactor shutdown time and vehicle-station separation distances necessary to adequately protect crew members present on the station during the return and subsequent orbital parking of nuclear-powered vehicles. In addition, scenarios were examined in which SS crew members might be involved in extravehicular activity (EVA) at various distances from the shutdown reactor of vehicles returning to LEO. The results from that study indicated that realistic scenarios exist which would allow the use of nuclear power sources in the vicinity of the station. Radiation doses to the SS crew could be maintained at safe levels solely by implementing proper and reasonable operational procedures. These constraints (parking distance and previous reactor shutdown time) were not considered to be severe and would not significantly impair the functionality of an evolutionary space station.

Nevertheless, the use of a portable, multifunctional radiation shield in LEO would both relax these constraints and reduce radiation doses to SS crew from natural space radiation sources in accordance with the "As Low As Reasonably Achievable (ALARA)" radiation protection philosophy. Consequently, the primary focus of the current study was to investigate combined implementation of time, distance, and shielding options to reduce crew exposures while adding operational flexibility to NASA mission planners.

PORTABLE RADIATION SHIELD - SUMMARY AND CONCLUSIONS

Most nuclear systems that interact with SS will not require a 4π man-rated shield to meet the radiation protection requirements of their own missions. For instance, the propellant tanks on the NTR Mars vehicle provide a large fraction of the crew shielding. Most of the reactors only utilize shadow or disk shields for the protection of the personnel and/or electronics associated with them. Thus, there may be little, if any, shielding between the reactor and SS crew during orbital operations in LEO. While access to the vehicle can be achieved with little radiological consequence through the use of time and distance considerations, the presence of a portable radiation shield in LEO which could be deployed between the reactor and the station would allow for rapid access to the vehicle upon its return. Furthermore, there will be periods when there are not any nuclear systems in the vicinity of SS. During such periods of time, the portable shield could be placed around the SS crew habitat modules in order to reduce the dose from natural sources. This would serve to increase the dose budget available for subsequent interactions with nuclear systems in LEO and would be consistent with the ALARA principle.

In this study, various laminated shield designs were explored in which two shield layers were considered: one of tungsten for use as the primary shield for fission product gamma-rays, and one of aluminum for use as the primary shield for trapped proton radiation fields. Additional design parameters included the source-to-dose-point separation (1-km parking scenario or a 50-m EVA scenario), the previous reactor shutdown prior to shield deployment (0 days or 30 days), and the target dose of interest (0.2 Sv, 0.05 Sv, or 0.01 Sv) (see Appendix A for a summary of radiation dose quantities and units). Whereas a variety of dual lamination shield designs were assessed, the pure tungsten shields were found to offer comparable dose reductions at a lower total mass per projected shield area. In its secondary use as a proton shield, the 0.2-Sv NEP shield designs were found to offer a greater than 10-fold reduction in the primary trapped proton flux at space station. Essentially no penetration was seen for the 0.05-Sv and the 0.01-Sv shields. For the NTR shields, calculations indicated that the 0.05-Sv shield design was needed for a greater than 10-fold reduction in the primary proton flux; a 100-fold decrease was seen for the 0.01-Sv shield. Furthermore, it was shown that the lamination order and composition at a given target dose can contribute no more than an additional factor of 2 in the reduction of the proton flux at space station. Mass savings with the tungsten shield might very well dominate any additional gains seen in proton dose reduction offered by the more complex and possibly costly Al/W or W/Al lamination designs. Pure tungsten shields are thus recommended for any implementation of a nuclear-vehicle portable shield in LEO.

MATERIAL ACTIVATION ON CO-ORBITING PLATFORMS

With the establishment of a transportation infrastructure in low earth orbit, nuclear reactors may be needed to meet the power requirements of exploration activities. Various scientific and/or operational platforms might use as their power source SP-100 reactors which would co-orbit with the space station. Mission planners would need to establish procedures for the maintenance of these facilities. One concern would be the activation of materials in tools used during in-orbit EVA operations. Scenarios may arise in which tools or other materials are left on the platform from work performed while the reactors are in a shutdown state. During subsequent restart of the reactors, these materials would be subject to a neutron flux whereby some constituent elements may be radioactivated. This induced radioactivity would serve as a source of radiation exposure to crew members who would latter retrieve the tools and bring them back to the station. In this portion of the study, calculations were made to provide a relative ranking of various metals with regard to their potential for radiation exposure to crew members under these circumstances.

A major conclusion from this segment of the study was that radioactivation of materials some 20 meters from the reactor within the shadow of the reactor shield complex will be of negligible radiological concern. Additional calculations showed that rather substantial radiological concerns may arise for some elements exposed to the unshielded neutron flux of the operating reactor in the radial direction. Elements of potential concern in this latter scenario include Au, Co, Ni, Ta, and possibly W and Zr.. For very long irradiations (several years), additional metal elements of concern would include Cu, Fe, Mg, Mn, and Zn.

References

Bolch, W. E., J. Kelly Thomas, K. Lee Peddicord, Paul Nelson, David T. Marshall, and Donna M. Busche, "A Radiological Assessment of Nuclear Power and Propulsion Operations near Space Station Freedom", NASA Contractor Report 185185, March 1990.

CHAPTER 2

RADIATION DOSE LIMITS FOR SS PERSONNEL

INTRODUCTION

This chapter presents current dose limits for radiation exposures to space workers during low-earth orbital missions. Since individuals at SS will receive a somewhat constant radiation dose from trapped protons and galatic cosmic rays (GCR), the difference between recommended dose limits and doses from natural space radiations can be defined as an "available radiation dose budget" to be assigned to each individual crew member. If necessary, this dose budget could then be expended through exposures to man-made radiation sources such as nuclear reactors, radioisotope sources, or even medical x-ray examinations. It is current radiation protection practice to keep such exposures "As Low As Reasonably Achievable" (ALARA) (ICRP 1977 and NCRP 1987). Nevertheless, mission planners should be cognizant of the operational limits imposed, not only by the ALARA principle, but by the use of these individual radiation dose budgets. Before introducing the radiation dose limits to space workers, the general considerations by which they are defined are discussed below.

RADIATION PROTECTION CONSIDERATIONS

Health effects of radiation exposure fall under two general classes: stochastic effects and nonstochastic effects. Nonstochastic effects are those for which severity of the effect increases with increasing radiation dose delivered above a certain threshold. This threshold dose can vary greatly between individuals. Examples of nonstochastic effects are cataracts, blood changes, and decreased sperm production in the male. Stochastic effects are those for which only the probability of occurrence increases with increasing radiation dose, the severity of the effect is dose independent, and a threshold dose level, if it exists, is close to zero. Consequently, any radiation exposure will have an associated level of risk, however small. The main stochastic effects of concern are cancer (malignant tumors and leukemia) and genetic effects.

By international agreement, the principal objectives of radiation protection are: (1) to prevent the occurrence of nonstochastic effects; and (2) to reduce the risk of stochastic effects to levels comparable to risks associated with traditionally "safe" occupations (ICRP

1977 and NCRP 1987). Three concurrent approaches are generally used to achieve these objectives. First, all activities resulting in radiation exposures must be justified in terms of perceived benefits and projected costs. Second, all radiation exposures must be kept to as low a level as is reasonably achievable. Within the ALARA principle, it is assumed that economic and societal factors are to be used to determine what effort of dose reduction is deemed "reasonable". Finally, all individual radiation doses must be kept below recommended and/or regulatory dose limits.

NCRP RECOMMENDED DOSE LIMITS

Table 2.1 gives radiation dose limits for NASA's space workers as currently recommended by the National Council on Radiation Protection and Measurements (NCRP) (NCRP 1989). These career limits correspond to a 3% lifetime excess risk of fatal cancer where a career is assumed to be approximately 10 years. For the blood forming organs (BFO), the career limits range from 1.0 Sv for females 25 years of age at first exposure to 4.0 Sv for males 55 years of age at first exposure. Annual and 30-day limits are also specified so as to prevent the occurrence of nonstochastic radiation effects. As indicated in the table, an individual may receive 0.5 Sv to the BFO in a given year of space activity, yet cannot receive more than one-half the annual limit within any one 30-day period.

These NCRP recommendation were adopted by NASA in December of 1989 with the understanding that the dose limits would apply only to low-earth orbital missions, and that they would serve a guidance criteria for exploratory class mission. In May of 1990, the recommendations were adopted by the Occupational Safety and Health Administration (OSHA) of the U.S. Department of Labor, the organization with regulatory authority over radiation exposures to NASA personnel. The dose limits are currently incorporated within NASA-STD-3000, "Man-Systems Integration Standards" (Section 5.7 on Ionizing Radiation), and in JSC-12820, "Space Shuttle Operational Flight Rules" (Section 14 on the Space Environment).

RADIATION DOSE BUDGETS FOR SS CREW MEMBERS

Two radiation dose budgets are defined in this report: LBAD-st and LBAD-lt. The acronym LBAD stands for Lower Bound on Available Dose and the suffixes "st" and "lt" stand for short-term and long-term exposures, respectively. This approach is based upon three main considerations. First, man-made radiation sources in space predominantly emit

neutron and gamma radiations. Individuals exposed to these radiation types will generally receive uniform whole-body doses; consequently, only the NCRP limits to the blood forming organs are used to define dose budgets. Second, to be somewhat conservative, only the reference "worst-case" natural dose rate at SS (0.05 Sv/mo) is used in their definitions. Third, in order to cover the range of scenarios by which man-made radiation exposures may occur, two exposure types and periods are considered.

The first type is a short-term, infrequent exposure occurring once during a particular 30-day period. Because the exposure is infrequent, the 30-day NCRP dose limit would apply to the individuals exposed (0.25 Sv in 30 days). An example would be exposure during extravehicular activity (EVA) near a shutdown reactor as part of the unloading of a Mars vehicle. The second exposure type corresponds to a long-term, continuous exposure to crew members during a maximum 6-month tour-of-duty at the station. Because the exposure is continuous, the annual NCRP dose limit would apply (0.50 Sv in 6 months). An example would be radiation exposure from an operating reactor on a co-orbiting platform.

The numerical values for LBAD-st and LBAD-lt are calculated as follows:

LBAD-st = (NCRP 30-day Limit) - (Worst-Case Natural Dose @ SS Over 30 Days)
= (0.25 Sv/mo) - (0.05 Sv/mo)
= 0.20 Sv in 30 days.

LBAD-lt = (NCRP Annual Limit) - (Worst-Case Natural Dose @ SS Over 6 Months)
= (0.50 Sv/yr) - (6 mo/yr) (0.05 Sv/mo)
= 0.20 Sv in 180 days.

It is strictly coincidental that both radiation dose budgets numerically equal 0.20 Sv. If the LBAD-lt is prorated uniformly over a full 180-day crew rotation period, only 0.033 Sv from man-made sources would be allowed within any 30-day period. Consequently, the LBAD-lt is a more restrictive dose budget than the LBAD-st.

USE OF RADIATION DOSE BUDGETS

Radiation exposure of crew members will be one of the primary factors determining the operational limits on space nuclear power sources employed in the vicinity of SS. The

range of "permissible" operations can thus be linked to a range of "permissible" man-made radiation exposures. The upper bound of this dose range will, of course, be governed by the NCRP dose limits. The lower bound will be governed by the ALARA principle. This raises the question of what is a "reasonably achievable" radiation dose from man-made sources in space. One useful definition would be to limit such doses to levels comparable to those received by the natural background. On earth, this is generally acceptable since background doses are typically very low. Although "background" doses in low earth orbit are much greater, this definition nevertheless is still valid since natural doses over typical staytimes are below recommended limits and radiation exposure is but only one of several risks presented to space workers. For the purposes of this report, therefore, the ALARA principle when applied to LEO operations will limit man-made radiation exposures to levels equaling natural doses under best-case conditions (0.01 Sv/mo).

Table 2.2 summarizes this range of "permissible" dose levels. For infrequent exposure events occurring sometime within a given 30-day period, the most permissive space nuclear power operations would result in crew members expending their LBAD-st radiation dose budgets and thus reaching the NCRP 30-day dose limit. The most restrictive operations will result in crew doses equaling one-month exposures from natural sources under best-case conditions. Similar arguments hold for long-term, continuous exposure events near or at the space station.

References

ICRP (1977) Recommendations of the International Commission on Radiological Protection, ICRP Publication 26, International Commission on Radiological Protection, Pergamon Press, New York, 1977.

NCRP (1987) Recommendations on Limits for Exposure to Ionizing Radiation, NCRP Report No. 91, National Council on Radiation Protection and Measurements, Bethesda, Maryland, June 1987.

NCRP (1989) Guidance on Radiation Received in Space Activities, NCRP Report No. 98, National Council on Radiation Protection and Measurements, Bethesda, Maryland, July 1989.

Table 2.1 Recommended Dose Limits for Space Workers.
(NCRP 1989)

Time Period	Dose Equivalent (Sv)		
	Blood Forming Organs	Lens of the Eye	Skin
Career	1.0 - 4.0	4.0	6.0
Annual	0.50	2.0	3.0
30-day	0.25	1.0	1.5

Table 2.2 Bounding Radiation Dose Levels for Exposures to Man-Made Radiation Sources in Space.

Radiation Protection Criteria to be Used	Exposure Type and Period	
	Short-Term, Infrequent (1 Month)	Long-Term, Continuous (6 Months)
NCRP Dose Limits (Upper Bound)	LBAD-st (0.2 Sv in 30 days)	LBAD-lt (0.2 Sv in 180 days)
ALARA Principle (Lower Bound)	1 Mo. Nat. @ SSF (BC) (0.01 Sv in 30 days)	6 Mo. Nat. @ SSF (BC) (0.06 Sv in 180 days)

CHAPTER 3

CALCULATIONAL METHODS FOR SOURCE TERMS AND SHIELDING STUDIES

INTRODUCTION

This chapter deals with the determination of the neutron and gamma source terms for both operating and shutdown reactors. NERVA- and SP100-class reactors were chosen for the Mars mission and SS operational scenarios investigated in an earlier study (Bolch et al. 1990), and the source terms for these reactors are developed in this chapter. The operating reactor neutron and gamma source terms are based upon values generated as part of the SP-100 and NERVA projects. The shutdown reactor gamma source terms are based upon an empirical relationship for gamma release rates from fission products and the operating source terms.

The methods employed in this analysis are approximate and the results are intended primarily to aid mission planning; the values predicted using these methods are probably accurate to within ±25%. It is certainly possible to perform these analyses in a rigorous fashion. A number of coupled neutron-gamma transport codes are available to compute the operating reactor source term. The ORIGEN2 code (Croff 1983 and RSIC 1987) can be employed to provide accurate estimates of the radioisotope inventory based upon a reactor's operational history. However, the level of effort required to develop the reactor models required to implement the transport codes is rather large and was not justified at the time this project was initiated. This area is currently being pursued as part of a follow-on project.

DESCRIPTION OF REACTORS

The two reference systems employed in this study are SP-100 and NERVA-class reactors. The SP-100 reactor, until very recently, was under development as part of the U.S. space program (Armijo et al. 1989, Deane et al. 1989 and Manvi and Fujita 1987). It has a baseline thermal power of 2.4 MW_t and employs a static thermoelectric power conversion subsystem to produce 100 kW_e of power. The basic design goals of the SP-100, however, call for scalability up to an order of magnitude higher power. For the purposes of this project, it was assumed that the reactor would generate 25 MW_t and utilize

an active conversion system (Rankine or Brayton cycle) in order to provide 5 MW of electrical power. The SP-100 is a small, compact, fast-spectrum reactor. It utilizes highly enriched uranium mononitride (UN) fuel, niobium - 1% zirconium (Nb-1Zr) cladding, and lithium (Li) coolant. The core vessel and structure are composed primarily of Nb-1Zr and the other materials employed in the core are also refractory alloys. Beryllium oxide (BeO) hinged reflector panels located on the outside periphery of the core are employed as the primary control mechanism. The entire core and reflector structure is enclosed in a conical carbon-carbon reentry shield. A layered tungsten (W), lithium-hydride (LiH) shadow shield is employed to decrease the radiation field at the user interface.

The NERVA (Nuclear Engine for Rocket Vehicle Application) reactor concept was developed during the U.S. space nuclear propulsion program, which ended in 1973 (Bohl et al. 1988, Haloulakos and Boehmer 1988 and Borowski et al. 1989). A NERVA derivative reactor (NDR) concept capable of producing electrical power and being employed for propulsion was under study for application to the U.S. Multimegawatt reactor program (Pierce et al. 1989 and Schmidt et al. 1988). There is not a single fixed NERVA reactor design; rather NERVA was a basic reactor technology demonstration program that incorporated a number of similar reactor designs such as the NRX and XE reactor series (Angelo and Buden 1985). The basic NERVA reactor concept consists of a solid graphite core with a hydrogen coolant. A variety of fuel element designs were tested as part of the NERVA program and the most highly developed of these were uranium dicarbide (UC_2) particles with a pyrolytic carbon coating contained in a graphite matrix and a UC-ZrC-C composite fuel. A niobium or zirconium carbide (NbC or ZrC) fuel element coating was employed to reduce erosion by the hydrogen propellant. Primary reactor control was achieved through the use of rotating drums located on the outside periphery of the core. The bulk of the core vessel consists mainly of aluminum and steel. Two separate shields were employed in the NERVA design (Aerojet General 1970). The first is inside the pressure vessel and designed to protect the engine components from excessive heating. A brim or disk shield at the top of the core composed of layered lead (Pb), LiH, and Boral (a B-C-Al compound) was designed to decrease the radiation field away from the reactor for manned missions. The propellant storage tank provides a substantial amount of radiation shielding for the crew. In this work, the NERVA reactor was assumed to have a peak power of 1575 MW_t and be capable of producing low levels of electrical power (approximately 100 kW_e).

OPERATING REACTOR NEUTRON AND GAMMA SOURCE TERMS

The operating reactor neutron and gamma source terms were not directly computed as part of this project, rather the values employed in this work were developed using data from the SP-100 and NERVA projects. As mentioned previously, developing the geometric and material models required to implement neutron and gamma transport codes in a meaningful fashion is a rather time-intensive task. This topic is being explored as part of a follow-on project.

A number of common radiation analysis models (CRAM) were developed in conjunction with the NERVA project; the values employed in this work were taken from one of these models (Aerojet General 1970 and Wilcox et al. 1969). The CRAM provides values in terms of equivalent point sources for various engine components. The radiation field in a direction perpendicular to the axis of the reactor-engine assembly (i.e. radially outward) is dominated by the reactor; activation of and scattering from engine and structural components represent a second-order contribution. The neutron and gamma spectra for the operating NERVA reactor are given in Tables 3.1 and 3.2, respectively. Employing the dose response functions given in Appendix B yields specific operating NERVA dose rates at a 1 meter separation distance in the radial direction from an equivalent point source of 30.6 Sv/sec/MW_t for neutrons and 14.5 Sv/sec/MW_t for gamma-rays.

Data on the neutron and gamma levels in and around an SP-100 operating at 2.4 MW_t for beginning-of-life (BOL) conditions were available from General Electric (Marcille 1989). The neutron and gamma fluxes on the periphery of the reactor at the axial midplane were scaled linearly with power to 25 MW_t to provide a radial source term. Values were also extracted for a location behind the shadow shield; these were not scaled with the thermal power since it was assumed that the shield thickness would be increased to achieve the same dose at the user plane. The neutron and gamma spectra for the operating SP-100 reactor are given in Tables 3.3 and 3.4, respectively. The specific operating SP-100 dose rates at a 1 meter separation distance in the radial direction from an equivalent point source were computed as 14.5 Sv/sec/MW_t for neutrons and 0.897 Sv/sec/MW_t for gamma-rays. For locations behind the shadow shield, the specific dose rates at a 1 meter separation distance from an equivalent point source are 2.85×10^{-4} Sv/sec/MW_t for neutrons and 1.00×10^{-2} Sv/sec/MW_t for gamma-rays.

The specific radial operating dose rates employed in this work and given above are summarized in Table 3.5. As can be seen in the table, the values for the SP-100 are substantially smaller than those for the NERVA; this is particularly true for the specific gamma dose rate. Several factors contribute to these differences. The types of materials employed in the SP-100 and NERVA reactors are quite different. The SP-100 is comprised primarily of high atomic number (Z) refractory alloys while most of the structure of the NERVA is aluminum or steel. High Z materials are much more effective in attenuating gamma radiation and this will tend to decrease and soften the gamma spectrum of the SP-100 relative to that of the NERVA. Secondly, the SP-100 is a small, compact reactor whereas the NERVA is both large and graphite-moderated. This will produce a fast (hard) neutron spectrum in the SP-100 relative to the NERVA's thermal or epithermal neutron spectrum. Gamma-rays will be produced as a consequence of the neutron thermalization (slowing down) process and this will occur to a larger degree in the NERVA. The relative amount of structural and control materials in these reactors will also play a role. The ratio of the core to vessel (including reflectors) radius for the SP-100 is approximately 0.56 at the core axial midplane, while this value is 0.74 for the NERVA. Thus, there is proportionally more structural material, and hence radiation interaction, with the SP-100 compared to the NERVA. In addition, the energy groups selected from the SP-100 and NERVA project reports are not consistent. Those employed for the NERVA were simply the values available in the literature. For the SP-100, however, this energy structure was initially requested by the authors. GE has the capability to provide a number of different energy group structures; a set more closely matching that employed with the NERVA was not obtained due to time constraints. Lastly, the computational methods employed by the SP-100 and NERVA project teams are not the same. The SP-100 project is employing current radiation transport codes and cross section libraries and this factor could introduce some difference in the operating dose rate values. As previously mentioned, the development of "in-house" capabilities to carry out direct computation of the radiation source terms on a consistent basis will be explored in a follow-on project.

SHUTDOWN REACTOR GAMMA SOURCE TERMS

The shutdown reactor gamma source strength was computed using the simple empirical relationship shown below (LaBauve et al. 1982):

$$f(t) = \sum_{j=1}^{11} \alpha_j e^{-\lambda_j t}$$

where f is the energy release rate per fission (MeV/fission/sec), t is the time since the fission occurred, and α_j and λ_j are empirical constants. Integrating with respect to both reactor operating and shutdown time yields the gamma energy release rate at the time of exposure. There are alternate periods of full and reduced power operation in the Mars mission scenarios employed in this work; each period of operation is treated separately and the source terms are summed to compute a total source. As discussed in Appendix C, there are a large number of such relationships available which vary in complexity and accuracy.

Once the total source has been computed, the gamma dose rate is computed using the simple relationship shown below:

$$\dot{H}_{\gamma_s} = \dot{H}_{\gamma_o}\left[\frac{P_{\gamma_s}}{P_{\gamma_o}}\right]$$

where H is the gamma dose rate and P is gamma energy release rate (power), the subscripts s and o denote shutdown and operating conditions, respectively. The operating reactor dose rates were discussed in the section above. The operating gamma power is taken to be a fraction of the total reactor power, as shown below:

$$\dot{H}_{\gamma_s} = \dot{H}_{\gamma_o}\left[\frac{P_{\gamma_s}}{f_\gamma P_o}\right]$$

Prompt gammas are emitted simultaneously with a fission event and contribute about 7 MeV to the approximately 200 MeV of recoverable energy released per ^{235}U fission event. Gammas are also emitted as a result of neutron capture events and contribute another 3 to 12 MeV per fission (Lamarsh 1966). Fission product gammas are emitted after the fission event as a result of the radioactive decay of fission products. If the operating reactor dose rate corresponds to BOL conditions, then fission product gammas will make only a minor contribution to the corresponding dose rate. A value of 0.065 was taken for f_γ in this work. This method presumes that the operating and shutdown gamma spectra are identical since the conversion between flux and dose is energy dependent, as discussed in Appendix B. While this condition is not strictly met, the chief differences are in the low energy end of the spectrum and the low energy gammas do not make a large contribution to the total dose.

GAMMA SHIELDING CALCULATIONS

When a shield material is placed within a gamma radiation field, the resulting dose rate behind the shield is comprised of two distinct components. The first is due to uncollided gamma photons which traverse the shield without interaction. This dose component decreases exponentially with the linear thickness of the shield material. The second component of the gamma dose rate is due to gamma photons which undergo scattering interactions within the shield. This latter component is accounted for by a parameter B called the buildup factor and is equal to the ratio of the total to the uncollided gamma energy flux at the dose point. Consequently, the dose rate for an extended shield is given as:

$$\dot{H} = B \cdot \dot{H}_{uncollided} = B \cdot \dot{H}_0 \cdot e^{-\mu x}$$

where $\dot{H}_0$ is the unshielded dose rate, μ is the linear attenuation coefficient for the gamma-ray energies of concern, and x is the linear thickness of shielding material.

Buildup factors are a function of the shield material, the linear shield thickness, the geometry of the irradiation (point source, broad beam, etc.), and the photon energy. They can be obtained either through measurement or Monte Carlo radiation transport calculations. In general, they can be used to provide estimates of required shielding thicknesses within error limits on the order of 10% or better (Chilton et al. 1984). To facilitate their use in shielding calculations, various empirical formulas have been devised to give buildup factors as a function of shield thickness. Three common functional forms for the buildup factor are (1) the Berger formula, (2) the Taylor formula, and (3) the geometric progression (GP) form. There is wide consensus that the GP form of the buildup factor is the best available form with regard to its ability to allow accurate interpolation of Monte Carlo buildup factor estimates (Trubey 1991). Consequently, this functional form was used in this research.

The GP functional form for the buildup factor is given as:

$$B(E,\mu x) = 1 + \frac{(b-1)\,(K^{\mu x} - 1)}{(K - 1)} \qquad \text{for } K \neq 1$$

$$= 1 + (b - 1)\,\mu x \qquad \text{for } K = 1$$

and $$K(\mu x) = c(\mu x)^a + d\,\frac{\tanh(\mu x/X_k - 2) - \tanh(-2)}{1 - \tanh(-2)}$$

where b is the value of the buildup factor at one photon mean-free-path ($1/\mu$) and K is the multiplication of dose (or flux) per mean-free-path. The latter equation represents the dependence of K on the number of mean-free-paths (μx). The variables a, b, d, and X_k are fitting parameters which depend on the photon source energy. Mass attenuation coefficients (μ/ρ) are given in Tables 3.6 and 3.7 for the SP-100 and NERVA operating gamma spectrum, respectively, for both aluminum and tungsten shielding materials. For the case of the scaled SP-100 gamma spectrum, Tables 3.8 and 3.9 give the geometric progression buildup factor coefficients for Al and W, respectively. Similarly, Tables 3.10 and 3.11 give these same values for the Al and W, respectively, in the case of the NERVA gamma spectrum.

The above formulation for the buildup factor is for a single material. In this study, a two-material laminated shield is investigated for use as a multipurpose, portable radiation shield in LEO. The following rule is used for estimating the composite buildup factor for a two-layered radiation shield. Let us define the thickness of the two different materials as x_1 and x_2, numbered in the direction from the source to the dose point. If $Z_1 < Z_2$, the overall buildup is approximately equal to the buildup factor B_2 for the higher-Z medium with the use of $\mu_1 x_1 + \mu_2 x_2$ as its argument. However, if $Z_1 > Z_2$, the overall buildup factor to use is the product $B_1(\mu_1 x_1)$ times $B_2(\mu_2 x_2)$. The laminations should each be at least one mean-free-path length thick, and the source photon energy is used as the energy argument for all tabulated values. Further discussion of this approach may be found in Chilton et al. (1984).

The gamma dose rate from a shutdown reactor, at a location behind a shield of linear thickness x, is thus computed using the following expression:

$$\dot{H}_{\gamma_s}^{Shielded} = \sum_E \overline{B(E,x_1 + x_2)} \cdot \dot{H}_{\gamma_{s,E}} \cdot e^{-\mu x_1} \cdot e^{-\mu x_2} ,$$

where $\dot{H}_{\gamma_{s,E}}$ is the unshielded dose rate due to gammas within energy group E. As discussed earlier, this source term can be obtained by scaling operating gamma source terms by the ratio of the shutdown to operating reactor power levels:

$$\dot{H}_{\gamma_{s,E}} = \dot{H}_{\gamma_{o,E}} \left[\frac{P_{\gamma_{s,E}}}{P_{\gamma_{o,E}}} \right] = \dot{H}_{\gamma_{o,E}} \left[\frac{P_{\gamma_s}}{P_{\gamma_o}} \right] .$$

These gamma-ray shielding techniques were incorporated into a FORTRAN shielding code SHIELD.FOR for use in assessing the dose reduction capabilities of various portable shield designs (see Appendix D). Input parameters include the vehicle type (NEP or NTR), the exposure period (4-hours for EVA and 6-months for vehicle parking scenarios), source-to-target distance, and the previous reactor shutdown time. Iterations are then performed giving the shielded cumulative dose as a function of Al and W lamination thicknesses and for both lamination orders.

PROTON SHIELDING CALCULATIONS

The assessment of the portable shield in its secondary application as a means of reducing background radiation doses to SS crew was performed in this work by considering the radiation transport of trapped protons within the various shielding designs. Fig. 3.1 shows the differential energy spectrum of trapped protons at an altitude of 450 km and an inclination of 28.5^0 as estimated by the AP-8 Min Model (NCRP 1989). As shown, the protons incident upon SS are relatively energetic and exhibit a fairly constant flux up to 100 MeV. The flux then drops two orders of magnitude over the range 100 MeV to 500 MeV.

As protons penetrate the shield material, they lose kinetic energy primarily through coulombic interactions giving rise to ionization and excitation of the shield medium. With far less frequency, however, the protons may occasionally collide with the nuclei of the shield material generating target fragments including neutrons, secondary gamma-rays, and additional protons. While these interactions are rare (generally one nuclear collision for every 10^9 electron interactions), the neutrons and gamma-rays thus produced can serve as additional sources of dose beyond the shield. For thick shields, of course, nuclear

interactions within the far regions of the shield would be the primary contributors to any additional exit flux of particles. Ideally, the generation of secondary target fragments would need to be simulated in a full assessment of the portable shield concept. Initially, the NASA Langely proton transport code BRYNTRN was investigated for use in this work (Wilson et al 1989). However, reliable estimates of fragmentation cross section are available only for low-Z materials, and thus interactions in high-Z media such as the tungsten lamination could not be modeled.

As a suitable alternative, a proton shielding code was written using proton range data obtained from ICRU Report 49 (ICRU 1993) (see Appendix D). Proton ranges in both aluminum and tungsten over the energies of interest are shown in Fig. 3.2 where ranges are expressed in units of density thickness (product of the linear distance and the material density). At a given proton kinetic energy, the range of the proton is shown to be consistently greater in tungsten (high-Z) than in aluminum (low-Z). The pattern can be understood by noting that the electron binding energies are generally greater in higher-Z media and thus the rate of energy loss (stopping power) at a given particle velocity is correspondingly lower. Consequently, a greater density thickness must be traversed by the proton in the higher-Z media to lose the same amount of initial kinetic energy.

The proton shielding code subdivides incident LEO proton spectra (Fig. 3.1) into multiple energy bins. Each incident proton is then followed within the first and second laminations of the portable shield as specified by the user; range data are then used to calculate the exit kinetic energy of the particle. Calculations are repeated for each incident proton energy and a total differential exit spectra is tabulated and normalized for comparison to the incident trapped proton spectra at SS.

References

Aerojet General (1970) NERVA Engine Reference Data, S130-CP-090290AF1, Aerojet General, Sacramento, CA, Sept. 1970.

Angelo, J.A., Jr. and D. Buden (1985) Space Nuclear Power, Orbit Book Co., Malabar, FL. pp. 177 - 96.

Armijo, J.S. et al. (1989) "SP-100, Technology Accomplishments," in Trans. of the Sixth Symposium on Space Nuclear Power Systems, CONF-890103--Summs., held in Albuquerque, NM, 8-12 January 1989, pp. 352 - 6.

Bohl, R.J., J.E. Boudreau and W.L. Kirk (1988) "History of Some Direct Nuclear Propulsion Developments since 1946," in Space Nuclear Power Systems 1987, M.S. El-Genk and M.D. Hoover, eds., Orbit Book Co., Malabar, FL, pp. 467 - 73.

Borowski, S.K., M.W. Mulac and O.F. Spurlock (1989) "Performance Comparisons of Nuclear Thermal Rocket and Chemical Propulsion Systems for Piloted Missions to Phobos/Mars," presented at the 40th Congress of the International Astronautical Federation, held in Malaga, Spain, 7-13 October 1989, paper IFA-89-027.

Chilton, A.B., J. K. Shultis, and R. E. Faw, *Principles of Radiation Shielding*, Prentice-Hall, Inc., 1984.

Croff, A.G. (1983) "ORIGEN2: A Versatile Computer Code for Calculating the Nuclide Compositions and Characteristics of Nuclear Materials," Nucl.Tech., 62: 335-52.

Deane, N.A. et al. (1989) "SP-100 Reactor Design and Performance," in Trans. of the Sixth Symposium on Space Nuclear Power Systems, CONF-890103--Summs., held in Albuquerque, NM, 8-12 January 1989, pp. 542 - 5.

Haloulakos, V.E. and C.B. Boehmer (1988) "Nuclear Propulsion: Past, Present, and Future," in Trans. of the Fifth Symposium on Space Nuclear Power Systems, CONF -880122--Summs., held in Albuquerque, NM, 11-14 January 1988, pp. 329-2.

International Commission on Radiation Units and Measurement, "Stopping Powers and Ranges for Protons and Alpha Particles," ICRU Report 49, Bethesda, Maryland, May 1993.

LaBauve, R.J., T.R. England, D.C. George and C.W. Maynard (1982) "Fission Product Analytic Impulse Source Functions," Nucl.Tech., 56: 322-39.

Lamarsh, J.R. (1966) Introduction to Nuclear Reactor Theory, Addison-Wesley Publ. Co., Reading, MA, pp. 103-4.

Manvi, R. and T. Fujita (1987) SP-100 Program: Users Handbook, Basic Configurational Tradeoffs, JPLD-4154 Issue 3, Jet Propulsion Lab., Pasadena, CA, June, 1987.

Marcille, T. (1989) Personal Communication, General Electric Aerospace, SP-100 Program, San Jose, CA, July 1989.

NCRP (1989) Guidance on Radiation Received in Space Activities, NCRP Report No. 98, National Council on Radiation Protection and Measurements, Bethesda, Maryland, July 1989.

Pierce, B.L., R.R. Holman and H.D. Kulikowski (1989) "Single NERVA Derivative Reactor Design Concept for Space Nuclear Electrical Power and Direct Propulsion," in Trans. of the Sixth Symposium on Space Nuclear Power Systems, CONF-890103--Summs., held in Albuquerque, NM, 8-12 January 1989, pp. 145 - 8.

RSIC (1987) RSIC Computer Code Collection, ORIGEN2: Isotope Generation and Depletion Code - Matrix Exponential Method, CCC-371, Radiation Shielding Information Center, Oak Ridge National Laboratory, Oak Ridge, TN, Nov. 1987.

Schmidt, J.E., J.F. Wett and J.W.H. Chi (1988) "The NERVA Derivative Reactor and a Systematic Approach to Multiple Space Power Requirements," in Trans. of the Fifth

Symposium on Space Nuclear Power Systems, CONF-880122--Summs., held in Albuquerque, NM, 11-14 January 1988, pp. 415 - 6.

Wilcox, A.D., B.A. Lindsey and M.A. Capo (1969) NERVA-Flight-Engine Common Radiation-Analysis Model (U), RN-TM-0583, Nuclear Division, Aerojet General, Sacramento, CA, May 1969.

Wilson, J.W., L. W. Townsend, J. E. Nealy, S. Y. Chun, B. S. Hong, W. W. Buck, S. L. Lamkin, B. D. Ganapol, F. Khan, and F. A. Cucinotta, BRYNTRN: A Baryon Transport Model, NASA-TM 2887, March 1989.

Table 3.1 Operating Equivalent NERVA BOL Neutron Flux in Radial Direction.

Group	Energy Range	Flux @ 1m (neutrons/cm^2/sec)
1	E < 0.4 eV	8.4E+13
2	0.4 eV < E < 1 MeV	3.7E+14
3	E > 1 MeV	1.1E+14

Table 3.2 Operating Equivalent NERVA BOL Gamma Flux in Radial Direction.

Group	Lower Energy (MeV)	Upper Energy (MeV)	Flux at 1 meter (gammas/cm^2/sec)
1	7.50	30.00	1.2E+12
2	7.00	7.50	2.1E+12
3	6.00	7.00	6.6E+12
4	5.00	6.00	1.9E+13
5	4.00	5.00	6.8E+13
6	3.00	4.00	1.7E+14
7	2.60	3.00	1.3E+14
8	2.20	2.60	2.0E+14
9	1.80	2.20	3.3E+14
10	1.35	1.80	5.5E+14
11	0.90	1.35	1.0E+15
12	0.40	0.90	2.4E+15
13	0.00	0.40	3.6E+15

Table 3.3 Operating Equivalent Scaled SP-100 BOL Neutron Flux.

Group	Lower Energy (MeV)	Upper Energy (MeV)	Flux at 1 meter (neutrons/cm^2/sec)	
			Radial Direction	Behind Shield
1	2.23	20.00	5.32E+11	1.24E+06
2	1.35	2.23	4.93E+11	7.22E+05
3	0.82	1.35	3.45E+11	6.82E+05
4	0.50	0.82	4.77E+11	6.37E+05
5	0.30	0.50	3.95E+11	4.68E+05
6	0.11	0.30	9.39E+11	7.54E+05
7	4.09E-02	1.11E-01	9.90E+11	4.60E+05
8	5.53E-03	4.09E-02	1.88E+12	9.21E+05
9	1.67E-04	5.53E-03	1.76E+12	1.50E+06
10	4.14E-07	1.67E-04	3.83E+11	1.80E+06
11	1.39E-10	4.14E-07	2.96E+10	9.92E+04

Table 3.4 Operating Equivalent Scaled SP-100 BOL Gamma Flux.

Group	Lower Energy (MeV)	Upper Energy (MeV)	Flux at 1 meter (gammas/cm^2/sec)	
			Radial Direction	Behind Shield
1	2.50	30.00	4.05E+11	4.14E+08
2	0.75	2.50	1.32E+12	1.08E+09
3	0.30	0.75	9.34E+11	1.07E+09
4	0.01	0.30	1.40E+12	5.86E+09

Table 3.5 Operating Equivalent SP-100 and NERVA Specific Dose Rates.

Reactor Type	Specific Dose Rate at 1 meter (Sv/sec/MWt)			
	Radial Direction		Behind Shadow Shield	
	Neutrons	Gammas	Neutrons	Gammas
NERVA	30.6	14.5	n/a	n/a
SP-100	14.5	0.897	2.85E-04	1.00E-02

Table 3.6 Mass Attenuation Coefficients for the Scaled SP-100 Gamma Spectrum

Group	Mean Energy (MeV)	Mass Attenuation Coefficient (cm^2/g)	
		Al	W
1	16.25	2.18E-02	5.51E-02
2	1.63	4.82E-02	4.76E-02
3	0.53	8.21E-02	1.22E-01
4	0.16	1.33E-01	1.45E+00

Table 3.7 Mass Attenuation Coefficients for the NERVA Gamma Spectrum

Group	Mean Energy (MeV)	Mass Attenuation Coefficient (cm^2/g)	
		Al	W
1	8.75	2.39E-02	4.57E-02
2	7.25	2.51E-02	4.37E-02
3	6.50	2.60E-02	4.27E-02
4	5.50	2.74E-02	4.14E-02
5	4.50	2.97E-02	4.05E-02
6	3.50	3.32E-02	4.03E-02
7	2.80	3.69E-02	4.11E-02
8	2.40	4.00E-02	4.24E-02
9	2.00	4.32E-02	4.37E-02
10	1.58	4.89E-02	4.82E-02
11	1.13	5.84E-02	6.01E-02
12	0.65	7.53E-02	9.71E-02
13	0.20	1.20E-01	7.38E-01

Table 3.8 GP Exposure Buildup Factor Coefficients for Aluminum
(Scaled SP-100 Gamma Spectrum)

Group	Mean Energy (MeV)	Geometric Progression Fitting Parameters (Al)				
		a	b	c	d	Xk
1	16.25	0.053	1.222	0.861	-0.0512	15.380
2	1.63	-0.044	1.836	1.210	0.0150	15.831
3	0.53	-0.082	2.260	1.466	0.0204	16.596
4	0.16	-0.061	2.854	1.377	0.0123	20.788

Table 3.9 GP Exposure Buildup Factor Coefficients for Tungsten
(Scaled SP-100 Gamma Spectrum)

Group	Mean Energy (MeV)	Geometric Progression Fitting Parameters (W)				
		a	b	c	d	Xk
1	16.25	0.012	1.618	1.381	-0.0477	13.475
2	1.63	0.011	1.423	0.986	-0.0204	14.066
3	0.53	0.093	1.307	0.687	-0.0504	13.998
4	0.16	0.352	1.233	0.166	-0.1069	14.832

Table 3.10 GP Exposure Buildup Factor Coefficients for Aluminum (NERVA Gamma Spectrum)

Group	Mean Energy (MeV)	Geometric Progression Fitting Parameters (Al)				
		a	b	c	d	Xk
1	8.75	0.033	1.311	0.911	-0.0288	13.561
2	7.25	0.029	1.411	0.923	-0.0253	13.299
3	6.50	0.027	1.460	0.929	-0.0245	12.718
4	5.50	0.022	1.505	0.945	-0.0198	11.615
5	4.50	0.016	1.568	0.966	-0.0161	11.560
6	3.50	0.002	1.640	1.016	-0.0095	11.505
7	2.80	-0.014	1.695	1.076	-0.0002	11.696
8	2.40	-0.023	1.738	1.115	0.0045	13.508
9	2.00	-0.032	1.781	1.153	0.0091	15.320
10	1.58	-0.045	1.843	1.218	0.0158	15.900
11	1.13	-0.061	1.958	1.308	0.0204	15.892
12	0.65	-0.079	2.168	1.432	0.0221	16.833
13	0.20	-0.074	2.762	1.455	0.0114	17.020

Table 3.11 GP Exposure Buildup Factor Coefficients for Tungsten (NERVA Gamma Spectrum)

Group	Mean Energy (MeV)	Geometric Progression Fitting Parameters (W)				
		a	b	c	d	Xk
1	8.75	0.051	1.469	1.050	-0.0740	14.131
2	7.25	0.060	1.440	0.980	-0.0818	14.221
3	6.50	0.058	1.414	0.970	-0.0789	14.293
4	5.50	0.053	1.395	0.964	-0.0746	14.140
5	4.50	0.034	1.378	1.001	-0.0580	13.830
6	3.50	0.016	1.385	1.030	-0.0411	13.570
7	2.80	0.013	1.410	1.020	-0.0348	13.416
8	2.40	0.010	1.419	1.016	-0.0274	13.408
9	2.00	0.007	1.428	1.012	-0.0200	13.400
10	1.58	0.012	1.422	0.983	-0.0204	14.156
11	1.13	0.035	1.432	0.885	-0.0264	13.590
12	0.65	0.074	1.354	0.741	-0.0412	13.695
13	0.20	0.347	1.155	0.248	-0.1966	13.680

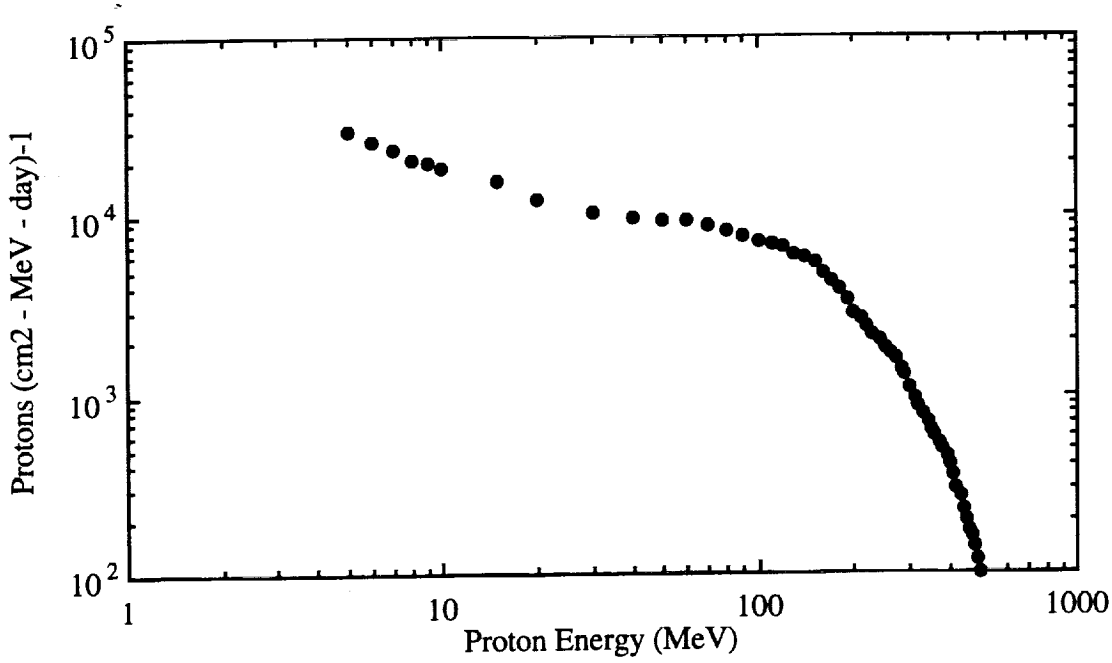

Figure 3.1 Differential Trapped Proton Spectrum at SS.

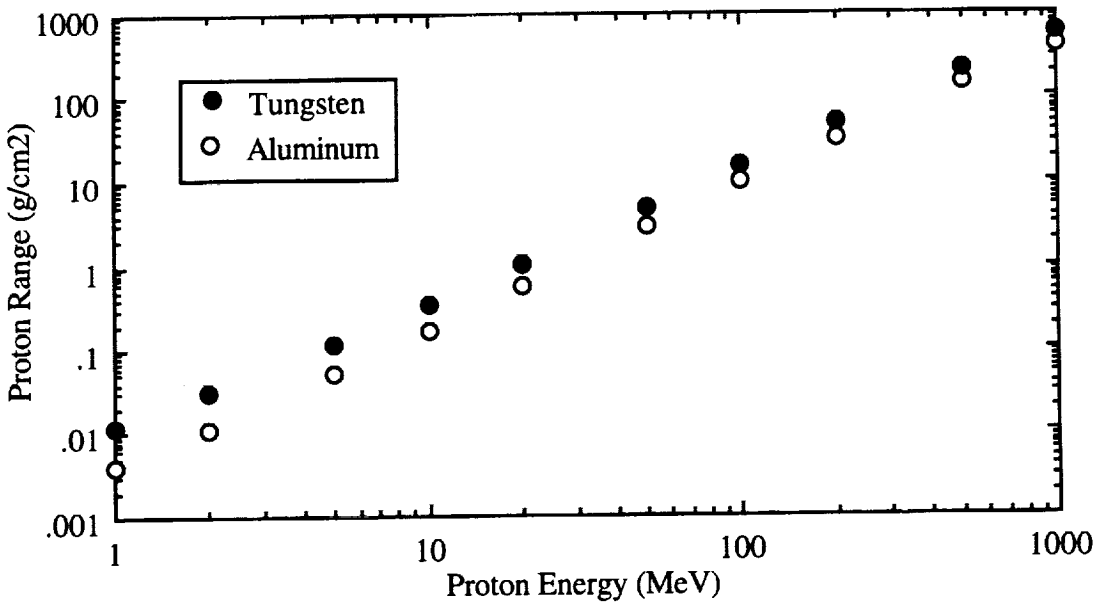

Figure 3.2 Proton Range within Aluminum and Tungsten Shield Materials

CHAPTER 4

DESIGN OPTIONS FOR A MULTIPURPOSE, PORTABLE RADIATION SHIELD

INTRODUCTION

In the previous study (Bolch et al. 1990), an analysis was performed of the radiological impact to SS crew of returning Mars vehicles. The work entailed the identification and characterization of likely Nuclear Electric Propulsion (NEP) and Nuclear Thermal Rocket (NTR) operational parameters, the computation of shutdown gamma source terms, and the subsequent calculation of radiation doses to the SS crew, either at the station or at the vehicle as part of an EVA. Estimates were then made of vehicle parking distances and shutdown times required to keep these doses within the allowable dose budget or to a level comparable to doses received from natural sources. Consequently, of the three fundamental techniques for reducing radiation exposures - time, distance, and shielding - only the first two were explored during the first phase of the study. In this second phase, further reductions in crew exposures via shielding options are explored as part of the multipurpose, portable radiation shield concept defined in Chapter 1.

MARS MISSION AND SS OPERATIONAL SCENARIOS

The two reference Mars mission scenarios employed in this work were developed based on discussions with the project staff at NASA Lewis Research Center (Stevenson and Willoughby 1989). The first consists of an NEP Mars cargo craft on a 1810-day round-trip to Mars departing from low earth orbit (LEO). It was assumed that an SP100-class reactor (Armijo et al. 1989 and Deane et al. 1989) would be employed. The reference SP-100 reactor has a baseline thermal power of 2.4 MW_t and employs a static thermoelectric power conversion subsystem to produce 100 kW_e of power. The basic design goals of the SP100, however, call for scalability up to an order of magnitude higher power. In the scenario employed here, it was assumed that the reactor would generate 25 MW_t and utilize a dynamic system (Rankine or Brayton cycle) in order to provide 5 MW of electrical power. The vehicle was assumed to spend 150 days in Mars orbit with the reactor operating at 0.4 MW_t and 373 days coasting with a housekeeping power level of 0.2 MW_t; for the remainder of the mission, the reactor was assumed to be operating at its

full rated power of 25 MW_t. The housekeeping power, 0.2 MW_t, was assumed to be available throughout the voyage.

The second Mars mission scenario consists of an NTR craft on a 486 day round-trip to Mars starting from LEO. The first portion of the mission, the trans-Mars insertion (TMI), is to be powered by a Phoebus-class reactor that would be discarded after Earth escape (Borowski et al. 1989 and Bohl et al. 1989). It was assumed that a NERVA-class reactor (Pierce et al. 1989 and Schmidt et al. 1988) operating at 1575 MW_t would be employed for the remainder of the mission. The NERVA-class reactor was assumed to be bimodal, providing both thermal power for propulsion and electrical power for housekeeping and mission requirements. The vehicle was assumed to spend 30 days in Mars orbit with the reactor operating at 0.4 MW_t and 456 days coasting at a housekeeping power level of 0.2 MW_t; for the remainder of the mission the reactor is to operate at its full rated power of 1575 MW_t. As with the NEP scenario, the housekeeping power is to be provided for the entire mission. The thermal power levels and duration of the mission phases for each of the mission scenarios are summarized in Tables 4.1 and 4.2.

The reactors were treated as point sources and no shielding from the vehicle structure, cargo, or onboard reactor shields was considered. This represents a "worst-case" scenario and is conservative. Activated core and vehicle components would also make a minor contribution to the shutdown gamma source strength, but were neglected in this work.

SHIELDING ANALYSIS FOR THE PARKING SCENARIO

As defined in the previous study (Bolch et al. 1990), the nuclear reactors on the returning Mars vehicles are assumed to be shutdown for some time period after arrival in LEO at a relatively large distance from SS. The craft are then towed or drift to within some variable parking distance of SS; it is at this time that the calculation of radiation dose to the SS crew begins.

Figs. 4.1 summarizes the results of phase one studies of the reference NEP vehicles. In this plot, the integrated six-month dose to the SS crew is plotted as a function of previous reactor shutdown time in days; additionally, each curve corresponds to a specific parking distance employed. In the case of the returning NEP vehicle, Fig. 4.1 shows that, for a parking distance of only 1 km, a previous reactor shutdown of ~180 days is required to insure that the integrated dose to the crew does not exceed radiation protection

requirements. A reactor shutdown time of greater than one year, however, is required at this parking distance if the dose contribution to the SS crew from the reactor is to equal that contributed by the natural space environment under best-case (BC) conditions. If, however, the parking distance of the returning NEP vehicle is increased to greater than 6 km, the parking dose is always less than the dose from natural space radiations, regardless of prior shutdown time.

The six-month parking dose from the NTR reactor is shown in Fig. 4.2. A reactor shutdown time of just under 90 days is required to meet the LBAD-lt criterion at a 1 km separation distance, a factor of 2 shorter than that for the NEP vehicle. Nevertheless, to allow parking distances greater than a few kilometers, a shutdown time of only one day is needed to allow the short-lived fission products produced during the EOC burn to decay sufficiently. A more detailed descriptions of these results can be found in NASA CR-185185 (Bolch et al. 1990).

While these results are highly encouraging for the use of either NEP or NTR in proximity operations within LEO, there may be situations where the vehicle would need to be docked to the station without a long delay after arrival to earth. Consequently, the availability of the portable shield concept may be important to station and mission operations.

In this analysis, shield design calculations were made under the following conditions. First, variable laminated shields were assumed from 100% Al to 100% W with both combinations of lamination order considered (Al followed by W indicated as Al/W versus W followed by Al indicated as W/Al). LiH was not considered in this study, although this material might effectively serve as an alternative to the low-Z aluminum component. Second, it was assumed that the vehicles were to be brought to within 1 km of the station. Third, two values of previous reactor shutdown were considered: 0 days and 30 days. Fourth, three 6-month target dose values were considered: 0.2 Sv, 0.05 Sv, and 0.01 Sv.

The first question explored was to what degree did the lamination order of tungsten and aluminum influence the dose reduction capabilities of the shield? Calculations performed and given in Figs. 4.3 and 4.4 for the NEP and NTR vehicles, respectively, show that the preferred order would differ depending upon which vehicle reactor type was employed. Each figure gives the required lamination thickness of tungsten (abscissa) and of aluminum (ordinate) needed to reduce the six-month integrated dose at a 1-km parking

distance to that indicated in the legend. In addition, a 0-day previous reactor shutdown period is assumed. In Fig. 4.3, the approximate nature of applying the buildup factor method to multilayer shields limits estimates to be made for only thick shields with lamination order Al/W for the NEP spectrum. Nevertheless, both figures indicate that the preferred (lower total mass) lamination orders would be tungsten followed by aluminum (W/Al) for the NEP shutdown spectrum of gamma-rays and aluminum followed by tungsten (Al/W) for the NTR shutdown spectrum of gamma-rays.

An intuitive understanding for this difference can be found in noting the energy spectral differences between the two reactor types. Figure 4.5 shows the relative beginning-of-life gamma flux in the radial direction for each reactor during operation. As shown, the spectrum of gamma energies for the NTR reactor (13 groups) is highly peaked at photon energies below 1 MeV, while that of the NEP reactor (4 groups) is relatively flat out to several tens of MeV. The corresponding mass attenuation coefficients for this range of photon energies are given in Fig. 4.6 showing the enhanced absorption capabilities of higher-Z materials such as tungsten at low photon energies due to photoelectric interactions. One can now image the high-flux, lower-energy photon spectrum from the NTR reactor incident upon a portable shield of either a W/Al or Al/W lamination order in which the Al thickness is of a fixed thickness. If the photons strike the tungsten layer first, they will be preferentially absorbed in photoelectric interactions due to the higher cross section in tungsten. The net effect will be a lower-flux, but slightly hardened energy spectrum entering the Al layer where the photoelectric effect is not as dominant as Compton scattering interactions. If, however, the photons were first incident upon the Al layer, the spectrum would be softened by Compton scattering, but not as greatly reduced in total flux. This softened spectrum would then enter the W layer, where photoelectric absorptions would have a larger effect in reducing the post-shield photon energy flux than in the previous case. Consequently, the preferred lamination order (lower total shield mass) for the NTR reactor gamma spectrum would be aluminum followed by tungsten (Al/W). Similar but opposite arguments may made for the NEP reactor shield. Nevertheless, Fig. 4.3 indicates the lamination order is less important for the NEP reactor spectrum, and thus a final portable shield design might well be fixed at a Al/W shield as dictated by the NTR calculations.

Final shielding designs for the NTR and NEP reactors are given in Figs. 4.7 and 4.8, respectively, for the vehicle parking scenarios. Each figure gives combinations of W and Al shield thickness needed to reduce the six-month integrated dose at 1 km to the values

indicated in the legend. The open symbols are for a 0-day reactor shutdown prior to dose integration, while the closed symbols are for a 30-day previous reactor shutdown. Fig. 4.7 shows that for a returning NEP reactor, a pure ~250 g cm^{-2} Al shield or a pure ~148 g cm^{-2} W shield would be required to reduce the six-month dose to 0.01 Sv (1 rem) without the added advantage of a previous reactor shutdown period. The corresponding shield requirements for the NTR reactor are ~190 g cm^{-2} of Al, ~162 g cm^{-2} of W, or various combinations as indicated in Fig. 4.8.

Also indicated in Figs. 4.7 and 4.8 are the reductions in shielding requirements at the various dose targets as the previous reactor shutdown time is extended from zero days to thirty days. There is a more substantial gain in dose reduction, and thus shielding reduction, for the case of the NTR reactor over that for the NEP reactor, which is again attributed to the large inventory of short-lived NTR fission products following the earth-orbital-capture burn. For the three six-month target doses of 0.01, 0.05, and 0.2 Sv, the extra 30 days of NTR reactor shutdown time results in reductions in required shielding of approximately 42%, 55%, and 77%, respectively. Since the NEP fission-product inventory consists of more long-lived isotopes, the corresponding percent reductions in shielding thickness are less: 12%, 17%, and 28%, respectively. Consequently, the additional 30-days of reactor shutdown time does not play as critical a role in reducing the shielding requirements of the NEP vehicle as it does for the arriving NTR vehicle.

SHIELDING ANALYSIS FOR THE EVA SCENARIO

Scenarios were also considered in which space station personnel might approach the vehicle in close proximity as in a 4-hour EVA along the vehicle proper. For these scenarios, Figs. 4.9 and 4.10 give the 4-hour integrated dose to crew members at 50, 100, and 200 meters from an unshielded shutdown reactor as a function of the prior reactor shutdown time (Bolch et al. 1990). Fig. 4.9 indicates that a shutdown time of at least 150 days is required to meet the LBAD-st dose criteria for a separation distance of 50 m. For this same shutdown time, separation distances of 100 m and 200 m would be needed to deliver the same dose as one month of natural exposure in LEO under worst-case and best-case conditions, respectively. Again, for the NEP vehicle, a reactor shutdown time of only 4 days would be required to meet the dose limits provided that the crew member remain greater than 200 m from the shutdown reactor.

In the case of the NTR vehicle, Fig. 4.10 shows that only 90 days is required to maintain EVA doses below the LBAD-st dose criteria. As with the NEP vehicle, only a relatively short shutdown time is needed (~ 6 days) to meet the dose limit criteria provided the separation distance exceeds 200 m. One may conclude then that additional shielding would be desirable in cases where work close to the reactor is necessary and operational conditions prohibit long reactor staytimes in higher orbit.

Shielding options for portable shield deployment at returning vehicles for the 50-m EVA scenario are given in Figs. 4.11 and 4.12 for the NEP and NTR vehicles, respectively. Fig. 4.11 shows that for a returning NEP reactor, a pure ~340 g cm^{-2} Al shield or a pure ~ 190 g cm^{-2} W shield would be required to reduce the four-hour integrated dose to 0.01 Sv without the added advantage of a previous reactor shutdown period. The corresponding shield requirements for the NTR reactor are ~405 g cm^{-2} of Al, ~ 310 g cm^{-2} of W, or various combinations as indicated in Fig. 4.12. As was seen in the parking scenarios, a substantial reduction in shielding requirements is gained if the NTR reactor is allowed to cool down for 30-days prior to any off-vehicle activity. Fig. 4.12 indicates that this additional 30-day period will allow shielding reductions of approximately 72%, 82%, and 91% for dose targets of 0.01 Sv, 0.05 Sv, and 0.2 Sv, respectively. While not as large as those for the NTR vehicle, the corresponding reductions for the NEP shielding requirements are still substantial: 32%, 44%, and 60%, respectively.

In comparing the shielding options for the parking scenarios (Figs. 4.7 and 4.8) to those of the EVA scenarios (Figs. 4.11 and 4.12), it appears that comparable shielding requirements would be needed for the both scenarios provided the reactors were allowed the 30-day shutdown period upon returning to LEO. If immediate access were needed to either vehicle, it appears that the shielding requirements necessary to insure that 4-hour EVA doses were below dose limits would be substantially greater than those needed to protect the SS crew from exposures to reactors on parked vehicles.

REDUCTIONS IN INCIDENT PROTON SPECTRUM AT SPACE STATION

One of the motivating factors for the establishment of a portable radiation shield in low earth orbit is the dual use of the shield in reducing trapped particle dose rates to station crew members during periods of little to no orbital vehicle operations. During these intermediate intervals, the shield may be positioned around the habitation modules of the station to reduce the natural background exposures from trapped particles, particularly the

lower proton radiation belts. By reducing the natural background exposures of crew members below the 0.01 to 0.05 Sv per month, the corresponding radiation dose budgets increase thereby permitting greater flexibility in the use of man-made radiation sources in low-earth-orbit operations.

Fig. 4.13 and its enlargement (Fig. 4.14) display the exiting proton spectra from four different portable radiation shield configurations in comparison to the ambient spectra at an altitude of 450 km and an inclination of 28.5^0. All four shield configurations correspond to designs which limit the 6-mo, 1-km parking dose to 0.2 Sv from a returning NEP with zero shutdown time. As shown in Fig. 4.13, all four shield combinations virtually remove the lower-energy component of the spectra (protons with kinetic energies less than 30 MeV), and slow down the higher-energy component from a measured maxima of 500 MeV to ~200 MeV. For the narrow range of proton energies exiting the shields, the incident proton flux is essentially reduced by a factor of 100. As stated earlier in Chapter 3, a full estimate of the reduction in dose rate cannot be directly assessed based upon these revised spectra without additional charged particle transport calculations; nevertheless, it appears that a substantial reduction in crew exposures from the natural space environment would be gained with the deployment of the portable shield around the station.

A further review of the differences in shield configuration as shown in Fig. 4.14 reveals that indeed shields of lower atomic number are more effective in attenuating the incident proton flux. For example, a pure Al shield will reduce the exiting flux of 100-MeV protons by a factor of ~2 compared to a pure W shield. Nevertheless, Fig. 4.14 indicates that there are not substantial differences between the four shield configurations in regard to their ability to reduce crew exposures to the trapped proton environment.

Additional analyses were conducted to look at reductions in differential proton spectra for six shield designs for each of the two nuclear-powered vehicles considered in this study. Fig. 4.15 shows a greater than 10-fold reduction in the differential proton spectra incident upon the space station when shielded with a pure tungsten or a pure aluminum 30-day, 0.2-Sv shield. Essentially no penetration is seen for shields designed at parking target doses of 0.05 Sv or 0.01 Sv. Because the shielding requirements for the NTR reactor at 30 days post-shutdown are less demanding than those for the NEP reactor (due to the lower fission product inventory), the corresponding reductions in the differential protons spectra are less dramatic for the NTR shield configurations as shown in Fig. 4.16. In this latter set, it is seen that a small but measurable distribution of exiting protons is present

even if the 0.01-Sv aluminum shield is deployed around the habitation modules. Nevertheless, a greater than 10-fold reduction is also seen for the 0.05-Sv NTR shields.

SUMMARY RECOMMENDATIONS ON SHIELD SELECTION

Table 4.3 summarizes the shielding results for both the NEP and NTR vehicle at three six-month integrated target doses of 0.2, 0.05, and 0.01 Sv and for a previous reactor shutdown of 30 days. Whereas a variety of dual lamination shield designs were assessed, this table only gives the required shielding thicknesses for a pure Al or a pure W design. As indicated earlier in Chapter 3, the tungsten shields offer comparable dose reductions at a lower total mass per projected shield area. When used as a proton shield, the 0.2-Sv NEP shield designs offer a greater than 10-fold reduction in the primary trapped proton flux at space station. Essentially no penetration is seen for the 0.05-Sv and the 0.01-Sv shields. For the NTR shields, the 0.05-Sv shield design is needed for a greater than 10-fold reduction in the primary proton flux; a 100-fold decrease is seen for the 0.01-Sv shield. Furthermore, the lamination order and composition at a given target dose can contribute no more than an additional factor of 2 in the reduction of the proton flux at space station. Mass savings with the tungsten shield might very well dominate any additional gains seen in proton dose reduction offered by the more complex and possibly costly Al/W or W/Al lamination designs. Pure tungsten shields would then be recommended for any implementation of a nuclear vehicle portable shield in LEO.

SHIELD DEPLOYMENT OPTIONS AT SPACE STATION

Deployment options for the portable radiation shields are complicated by the fact that the size requirements for shielding the station, shielding the NTR reactor, and shielding the NEP reactor vary considerably. The habitation modules for the station are cylindrical in shape with a length of ~13.41 m and an outer radius of ~2.13 m. The sleeping quarters occupies approximately one-half of this length or 6.70 m. The NERVA-class reactor of the NTR vehicle can be effectively encompassed by a cylindrical shield 4.17 m in length with an inner radius of 1.06 m. The SP-100-class reactor of the NEP vehicle at a rated thermal power level of 25 MW could be effectively shielded in the radial direction by a cylindrical shield of only 0.97 m in height with an outer radius of 0.39 m. Total 4π shielding geometry would most likely pose unnecessary difficulties in deployment and redeployment of the shield. The size and mass of a multipurpose, portable radiation shield in LEO would thus be dictated by the requirements for deployment over the larger NTR reactor.

As an example, consider the shielding mass requirements for the NTR reactor using the dosimetry estimates discussed previously in this Chapter. The total shield volume for the NTR reactor can be estimated as:

$$V_{shield} = \pi r_o^2 h - \pi r_i^2 h = \pi h\left[(r_i + t)^2 - r_i^2\right] = \pi h\left[2r_i t + t^2\right] ,$$

where r_0 and r_i are the outer and inner radius of the shield, respectively, h is the length of the shield, and t is the shield's linear thickness. For the NTR reactor, r_i is 1.06 m and h is 4.17 m. Furthermore, a pure tungsten NTR shield with a density thickness of 53 g cm^{-2} (corresponding to a 6-mo integrated dose to the station crew of 0.05 Sv) would have a linear thickness of the shield would be 2.75 cm of W. Consequently, the total shield volume would be 773,663 cm^3 giving it a total mass of 14.9 MT. For maximum flexibility, the shield could be constructed from rectangular panels of tungsten 2 m in length and 1 m in width. The total number of panels, N, needed for NTR deployment would thus be given as ratio of the total shield surface area to the area per panel:

$$N = \frac{S_{shield}}{A_{panel}} = \frac{2\pi(106\ cm)(417\ cm)}{(200\ cm)(100\ cm)} = 13.8 \approx 14 \text{ panels.}$$

When the NTR shield is subsequently deployed at the station during times of little or no vehicular activity in LEO, a greater number of panels would be needed. In one configuration, the total shield length could be kept constant at 4.17 m, thus shielding (417 cm / 670 cm) or 62% of the crew habitation module. Since the inner radius of the space station shield is essentially twice that of the NTR configuration (2.13 cm versus 1.06 cm), approximately 28 panels would be needed for station deployment. If the total shield mass were held constant, the thickness of the panels at space station would thus be limited to one-half of the 2.75 cm of W at the NTR vehicle, or ~1.38 cm. Under this scenario, each panel could be limited to 1.38 cm in thickness in which case the NTR shield would consist of a double wrapping of 14 pairs of shielding panels, while the space station shield would consist of a single wrapping of 28 single, 1.38-cm thick panels. Finally, the density thickness of the shield in its space station configuration would fall from 53 g cm^{-2} to ~27 g cm^{-2}; nevertheless, the data shown in Fig. 4.16 indicates that the station crew would still enjoy a factor of 10 reduction in the incident proton flux.

A similar analysis can be made of the mass requirements for NEP shield deployment. For a cylindrical shield 97 cm in length, 39 cm in its inner radius, and having a density thickness of 88 g cm^{-2} (see Table 4.3), the shield volume and mass would thus be 114,724 cm^3 and 2.21 MT, respectively. If the full complement of NTR shield panels were available, a maximum of (14.9 MT / 2.21 MT) or 6-7 NEP reactors could be shielded simultaneously. Although the scenario examined in this project envisioned a single-reactor NEP vehicle, current vehicle designs being explored at NASA Lewis envision multiple reactor NEP configurations; consequently, two of these three-reactor "hydra" NEP vehicles could be completely shielded with the 14.9 MT of tungsten currently available in LEO.

References

Armijo, J. S. et al. (1989) "SP-100, Technology Accomplishments," in Transactions of the Sixth Symposium on Space Nuclear Power Systems," CONF-890103, Albuquerque, New Mexico, January 8-12, 1989, pp. 253-356.

Bohl, R.J., J.E. Boudreau and W.L. Kirk (1988) "History of Some Direct Nuclear Propulsion Developments since 1946," in Space Nuclear Power Systems 1987, M.S. El-Genk and M.D. Hoover, eds., Orbit Book Co., Malabar, FL, pp. 467 - 73.

Bolch, W. E., J. Kelly Thomas, K. Lee Peddicord, Paul Nelson, David T. Marshall, and Donna M. Busche, "A Radiological Assessment of Nuclear Power and Propulsion Operations near Space Station Freedom", NASA Contractor Report 185185, March 1990.

Borowski, S. K., M. W. Mulac, and O. F. Spurlock (1989) "Performance Comparisons of Nuclear Thermal Rocket and Chemical Propulsion Systems for Piloted Missions to Phobos/Mars", presented at the 40th Congress of the International Astronautical Federation, held in Malaga, Spain, October 7-13, 1989, paper IFA-89-027.

Deane, N.A. et al. (1989) "SP-100 Reactor Design and Performance", in Transactions of the Sixth Symposium on Space Nuclear Power Systems," CONF-890103, Albuquerque, New Mexico, January 8-12, 1989, pp. 542-545.

Pierce, B.L., R.R. Holman and H.D. Kulikowski (1989) "Single NERVA Derivative Reactor Design Concept for Space Nuclear Electrical Power and Direct Propulsion," in Trans. of the Sixth Symposium on Space Nuclear Power Systems, CONF-890103--Summs., held in Albuquerque, NM, 8-12 January 1989, pp. 145 - 8.

Schmidt, J.E., J.F. Wett and J.W.H. Chi (1988) "The NERVA Derivative Reactor and a Systematic Approach to Multiple Space Power Requirements," in Trans. of the Fifth Symposium on Space Nuclear Power Systems, CONF-880122--Summs., held in Albuquerque, NM, 11-14 January 1988, pp. 415 - 6.

Stevenson, S. and A. Willoughby (1989) Personal Communication, NASA Lewis Research Center and Analex Corporation, Cleveland, Ohio, September 1989.

Table 4.1 NEP Mission Scenario Description.

Mission Phase	Duration (days)	Power (MWth)
Earth Spiral-Out (from 450 km)	443	25
Heliocentric to Mars		
1st Portion: Thrust	253	25
2nd Portion: Coast	162	0.2
3rd Portion: Thrust	85	25
Mars Spiral-In	86	25
Mars Operations	150	0.4
Mars Spiral-Out	39	25
Heliocentric to Earth		
1st Portion: Thrust	74	25
2nd Portion: Coast	211	0.2
3rd Portion: Thrust	68	25
Earth Spiral-In (to 450 km)	239	25
Earth Orbit Arrival	Variable	Reactor Shutdown

Table 4.2 NTR Mission Scenario Description.

Mission Phase	Duration (days)	Power (MWth)
Trans-Mars Insertion (TMI)	(1st stage)	(1st stage)
Coast To Mars	286	0.2
Mars Orbital Capture (MOC)	0.028	1575
Mars Operations	30	0.4
Trans-Earth Insertion (TEI)	0.024	1575
Coast To Earth	170	0.2
Earth Orbital Capture (EOC)	0.016	1575
Earth Orbit Arrival	Variable	Reactor Shutdown

Table 4.3 Summary of portable shield requirements for NEP and NTR vehicles corresponding to a previous 30-day reactor shutdown period.

Dose Target (Sv)	NEP		NTR	
	Al (g/cm2)	W (g/cm2)	Al (g/cm2)	W (g/cm2)
0.2	76	48	15	18
0.05	140	88	59	53
0.01	220	132	108	96

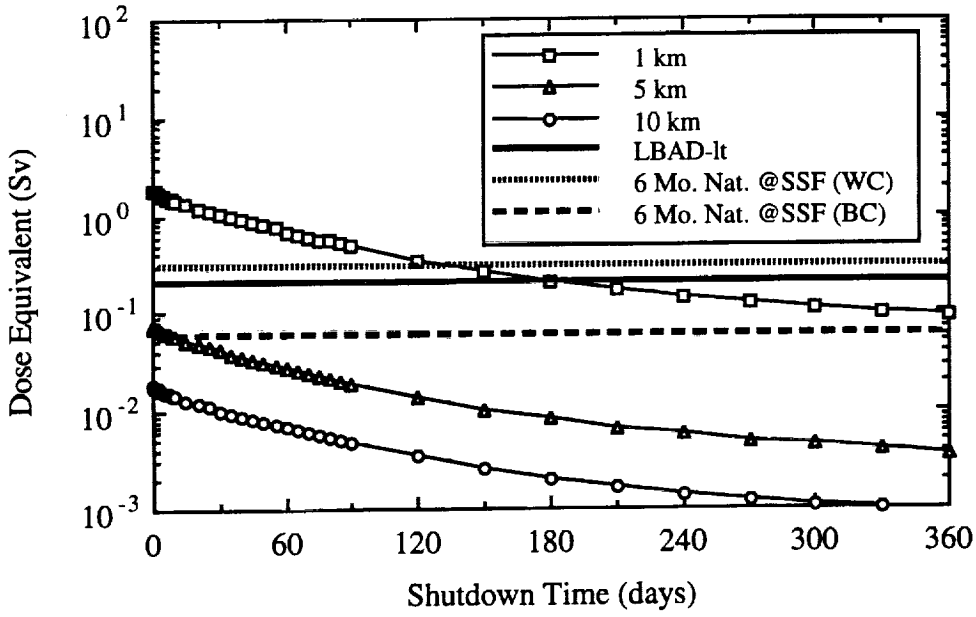

Figure 4.1 Shutdown NEP, 6 Month, Outside Shield, Parking Distance Curves.

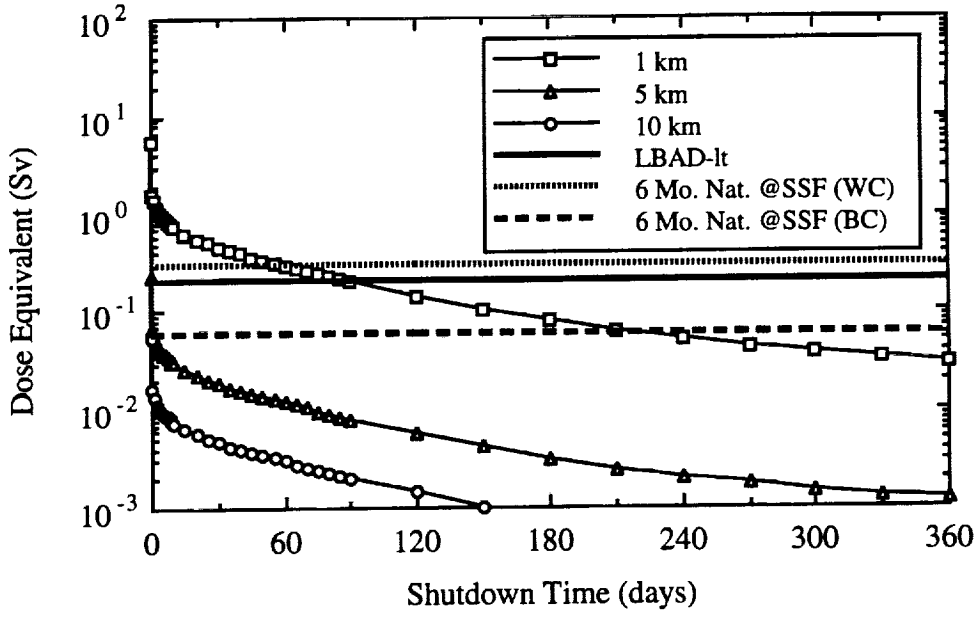

Figure 4.2 Shutdown NTR, 6 Month, Outside Shield, Parking Distance Curves.

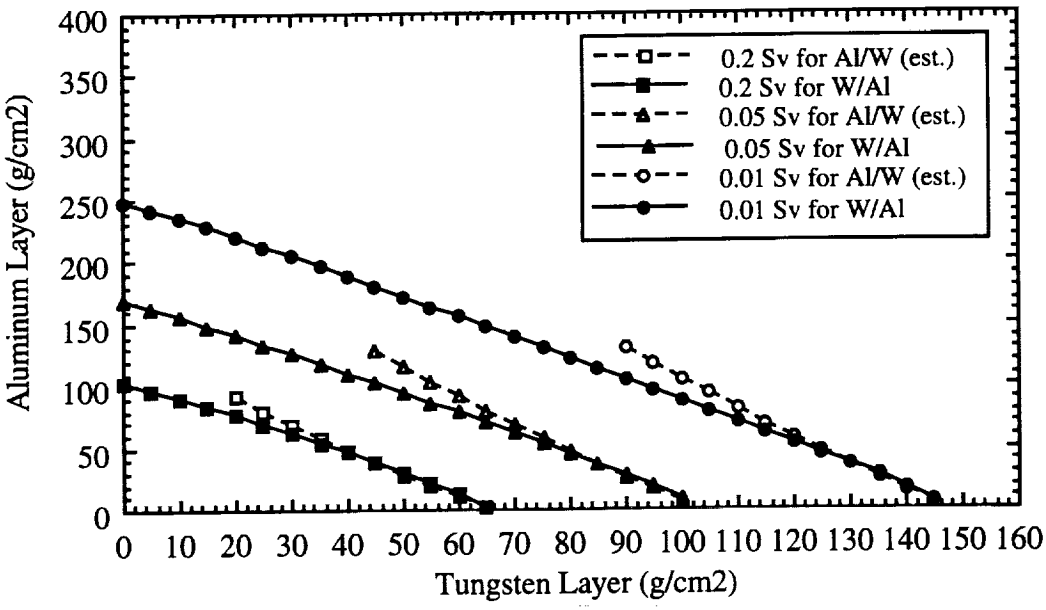

Figure 4.3 Out-of-Shadow Shielding Requirements for a Shutdown NEP. (6-Month Dose, 1-km Parking Distance, 0-Days Shutdown)

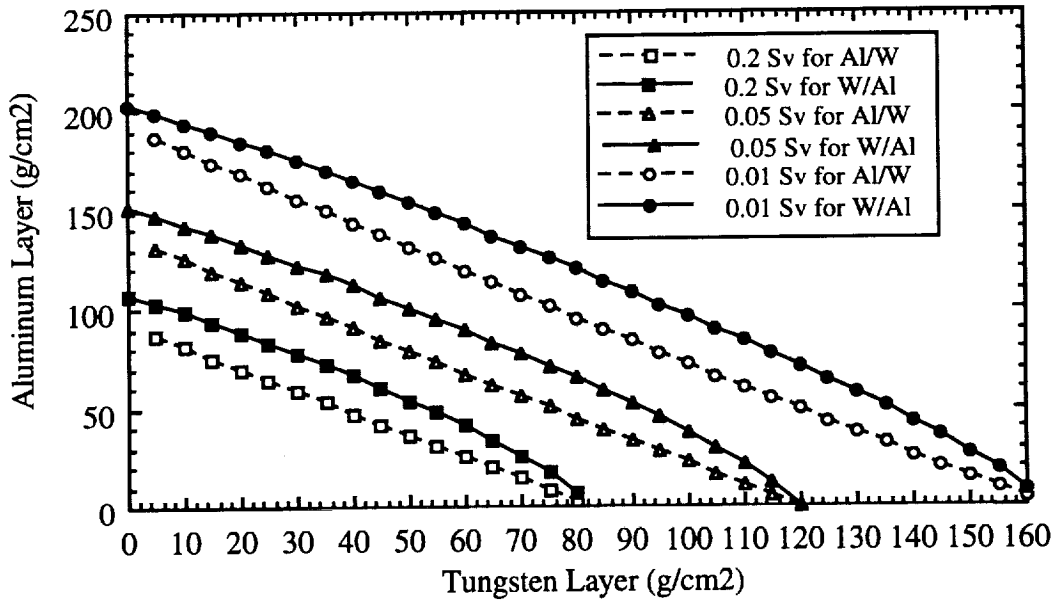

Figure 4.4 Out-of-Shadow Shielding Requirements for a Shutdown NTR. (6-Month Dose, 1-km Parking Distance, 0-Days Shutdown)

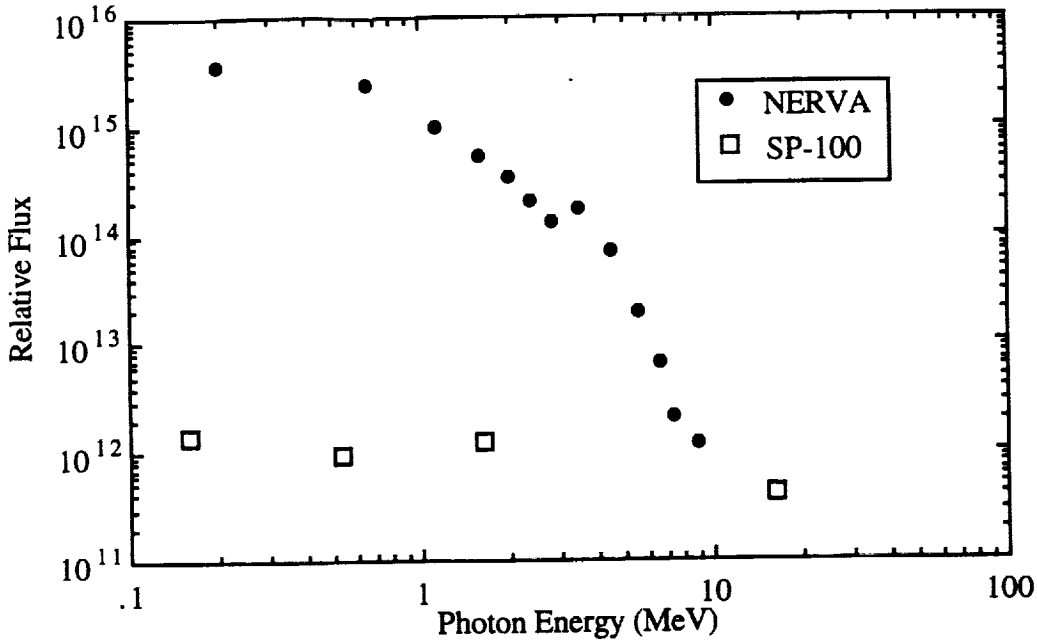

Figure 4.5 Operating Equivalent BOL Gamma Flux for the NERVA and Scaled SP-100 Reactors in the Unshielded, Radial Direction.

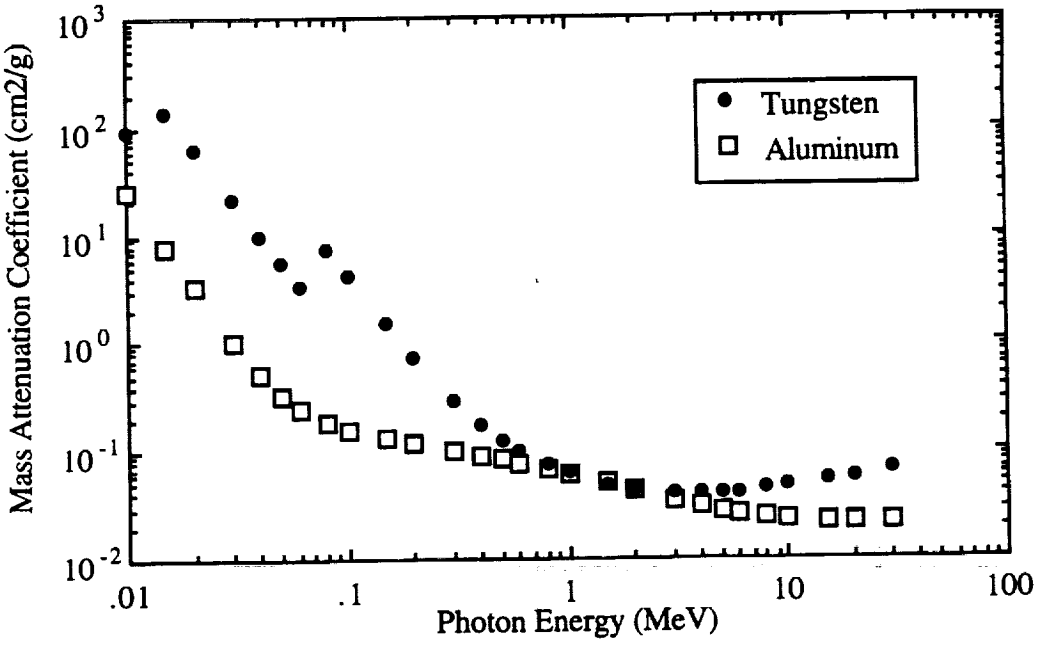

Figure 4.6 The Total Photon Interaction Cross Section for Al and W.

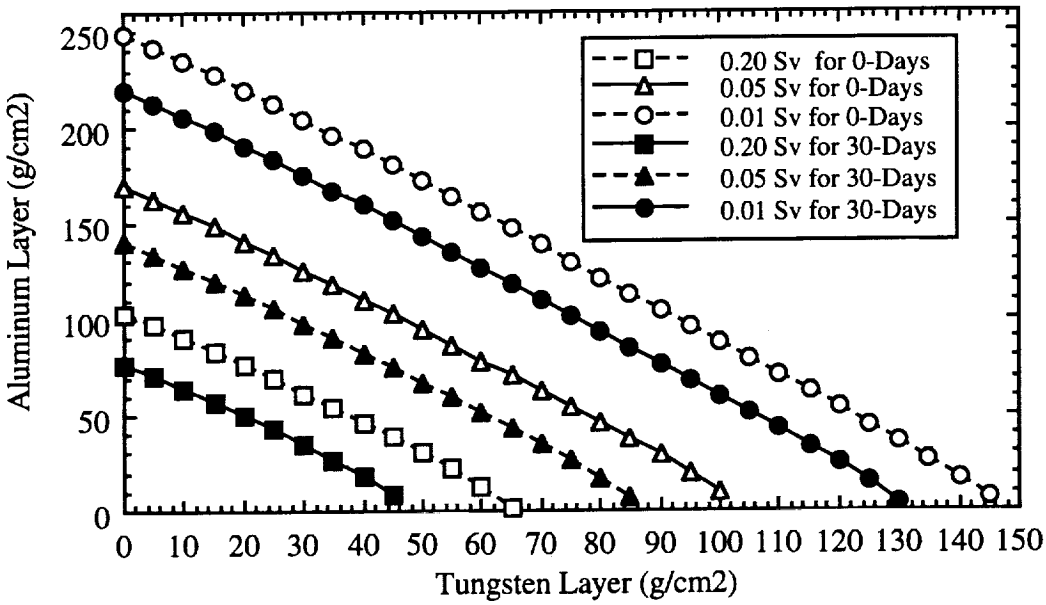

Figure 4.7 Out-of-Shadow Shielding Requirements for a Shutdown NEP. (6-Month Isodose Curves @ 1-km Parking Distance)

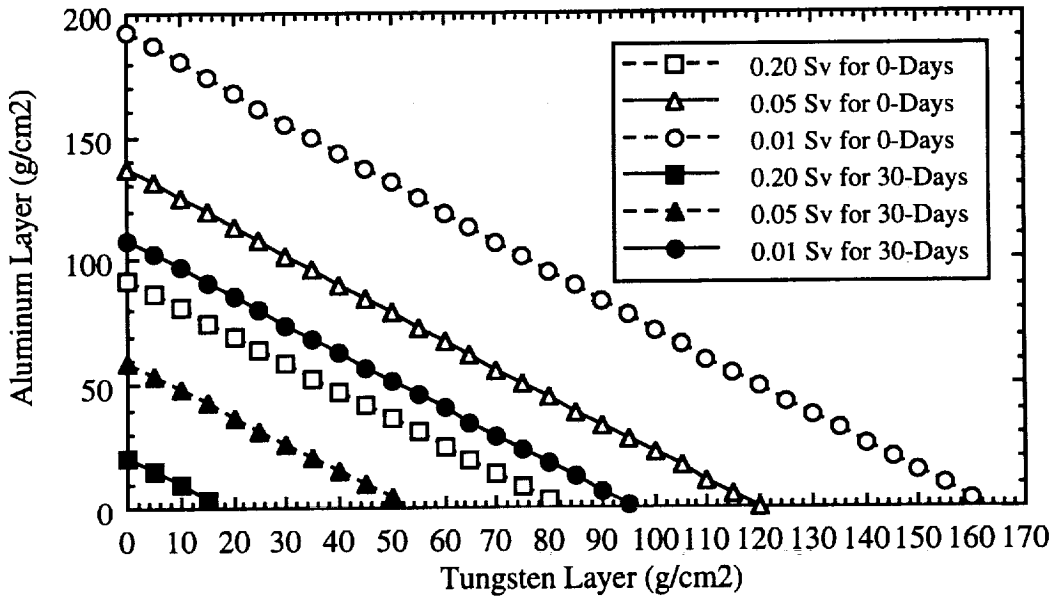

Figure 4.8 Out-of-Shadow Shielding Requirements for a Shutdown NTR. (6-Month Isodose Curves @ 1-km Parking Distance)

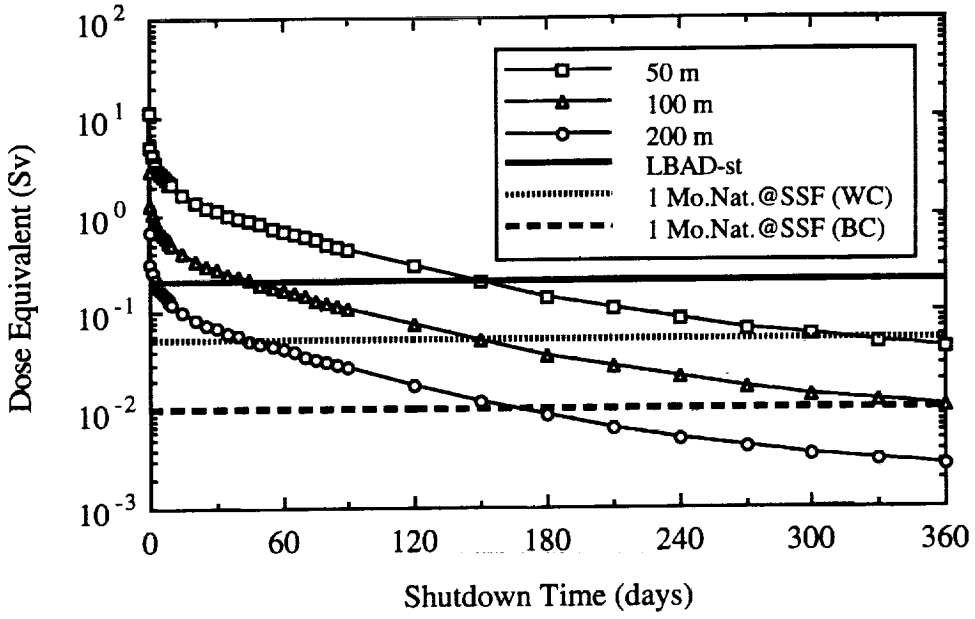

Figure 4.9 Shutdown NEP, 4 Hour EVA, Outside Shield, Separation Distance Curves.

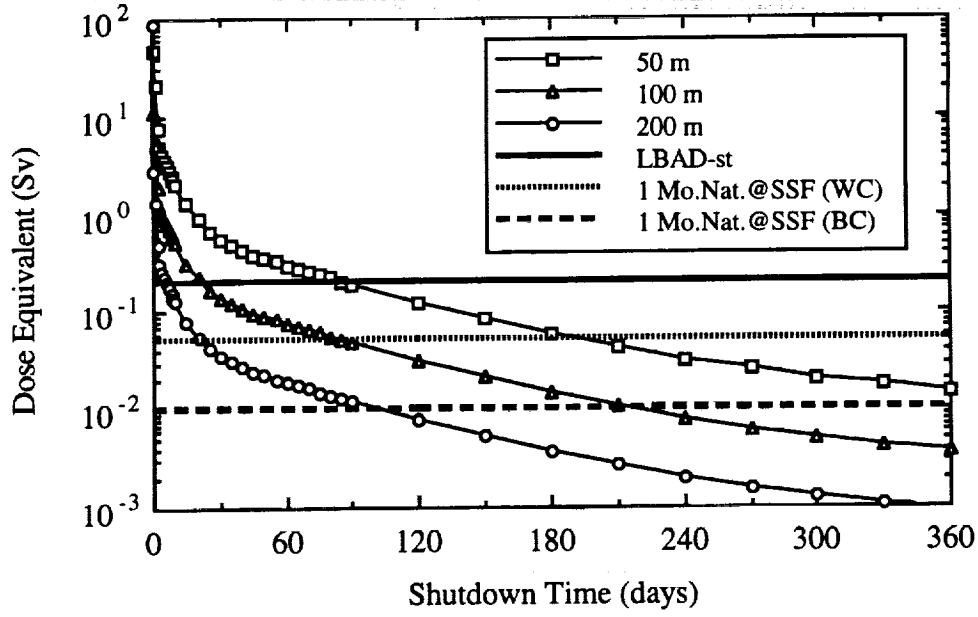

Figure 4.10 Shutdown NTR, 4 Hour EVA, Outside Shield Separation Distance Curves.

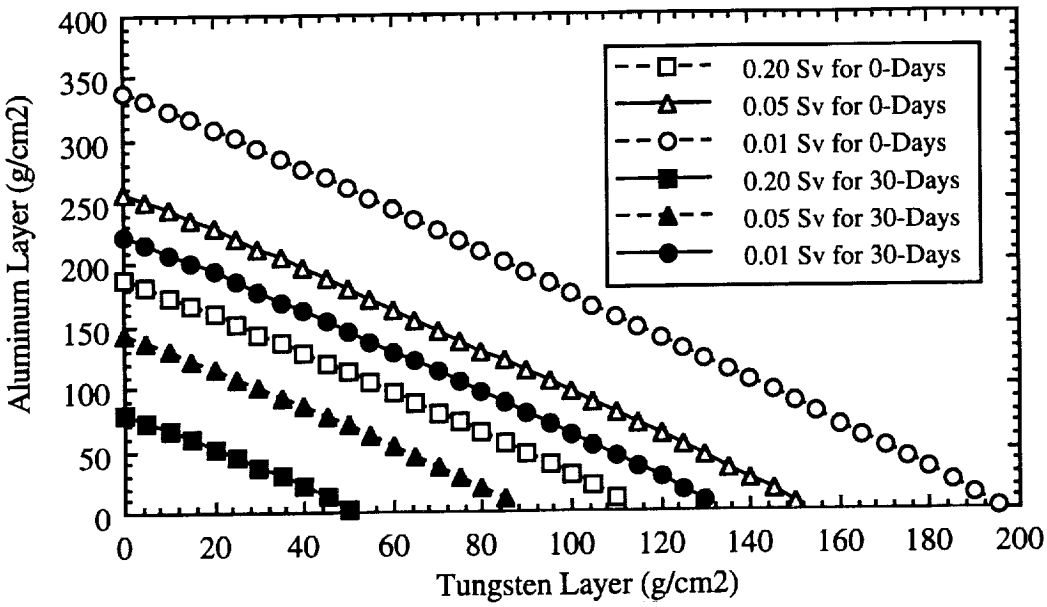

Figure 4.11 Out-of-Shadow Shielding Requirements for a Shutdown NEP. (4-Hour EVA Isodose Curves @ 50-m from Reactor)

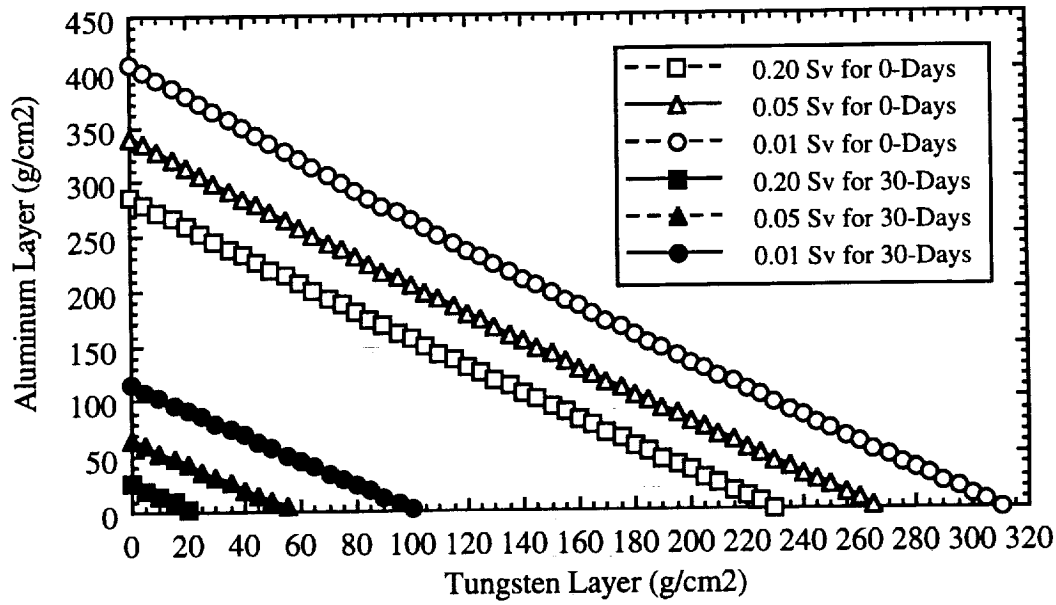

Figure 4.12 Out-of-Shadow Shielding Requirements for a Shutdown NTR. (4-Hour EVA Isodose Curves @ 50-m from Reactor)

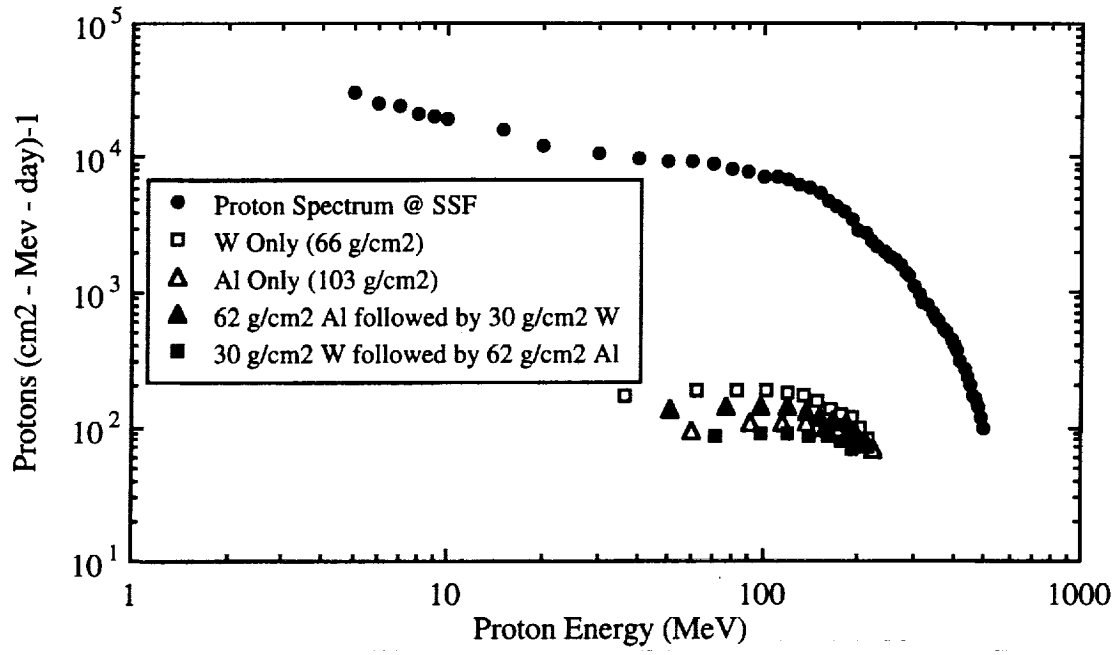

Figure 4.13 Reduction in Differential Proton Energy Spectrum @ SS Shield Design: (NEP, 6-Mo Dose of 0.2 Sv, 0-Day Shutdown)

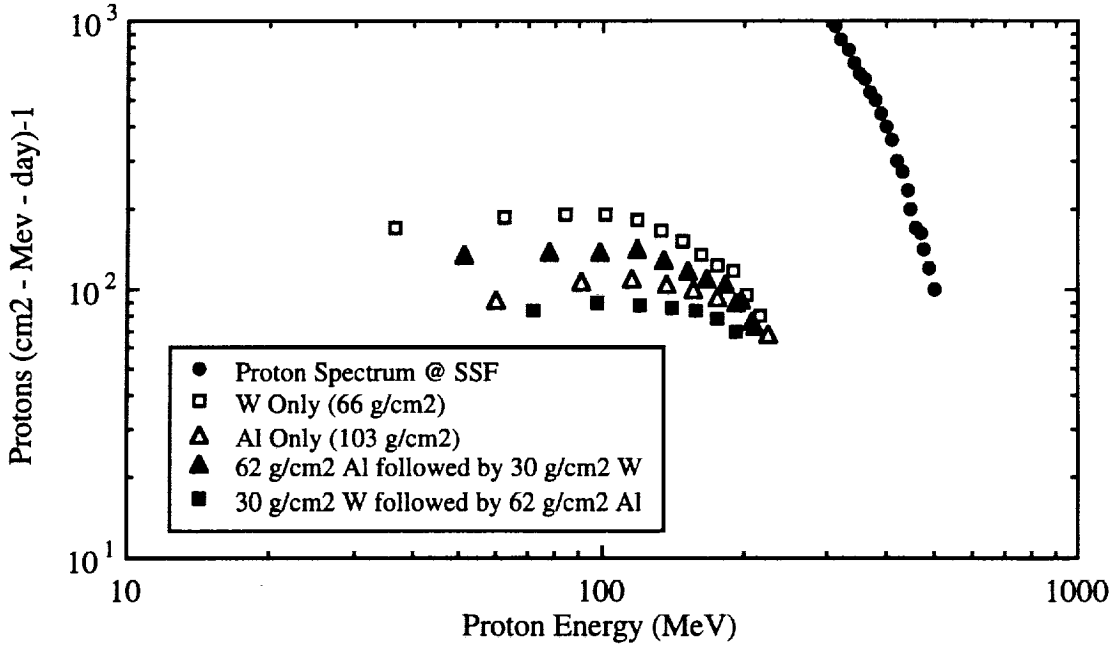

Figure 4.14 Expanded View of Fig. 4.13.

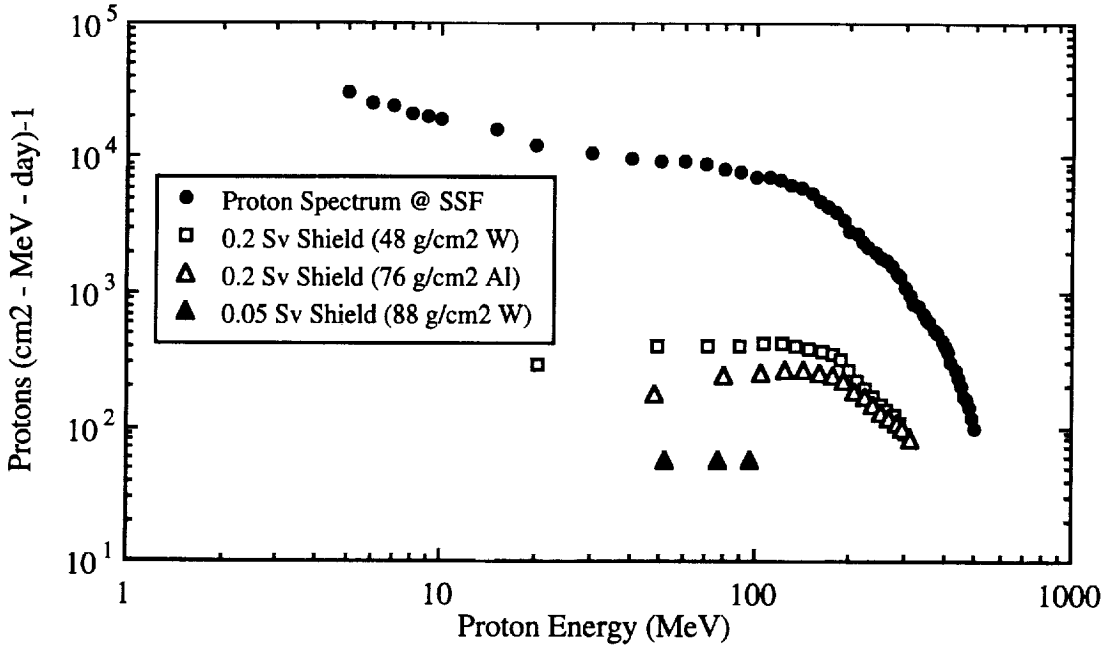

Figure 4.15 Reduction in Differential Proton Energy Spectrum @ SS Shield Design: (NEP, 6-Mo Doses Levels, 30-Day Shutdown)

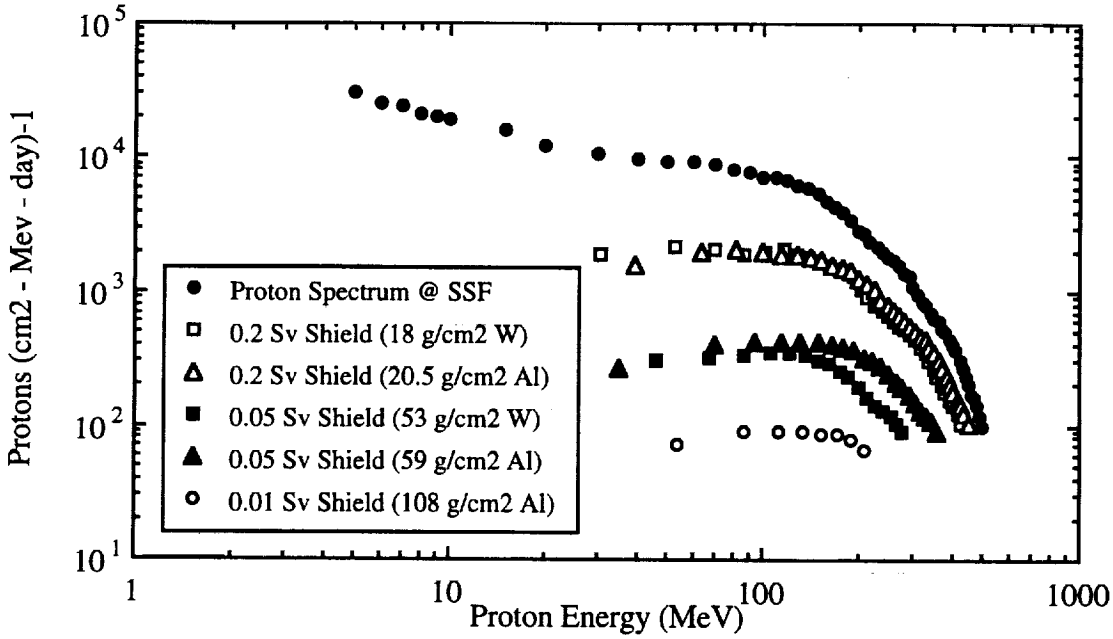

Figure 4.16 Reduction in Differential Proton Energy Spectrum @ SS Shield Design: (NTR, 6-Mo Doses Levels, 30-Day Shutdown)

CHAPTER 5

RADIATION CONCERNS FOLLOWING MATERIAL ACTIVATION ON CO-ORBITING NUCLEAR PLATFORMS

INTRODUCTION

With the establishment of a transportation infrastructure in low earth orbit, nuclear reactors may be needed to meet the power requirements of exploration activities. Various scientific and/or operational platforms might use as their power source SP-100 reactors which would co-orbit with the space station. Mission planners would need to establish procedures for the maintenance of these facilities. One concern would be the activation of materials in tools used during in-orbit EVA operations. Scenarios may arise in which tools or other materials are left on the platform from work performed while the reactors are in a shutdown state. During subsequent restart of the reactors, these materials would be subject to a neutron flux whereby some constituent elements may be radioactivated. This induced radioactivity would serve as a source of radiation exposure to crew members who would latter retrieve the tools and bring them back to the station. It would be helpful to mission planners to have a relative ranking of various metals with regard to their potential for radiation exposure to crew members under these circumstances.

METHODS OF ANALYSIS

To address these questions, calculations of induced activity were made for sixteen different metals exposed to neutron fields around an operating SP-100 reactor. For each metal, two sample configurations, two irradiation positions, and three irradiation times were considered. Sample configurations included both a fixed volume of 125 cm^3 (a cube 5-cm on a side) or a fixed mass (1-gram sample). While these choices are somewhat arbitrary, they do allow for a relative comparison between various types of metals of abundance in tools or other objects subjected to the reactor neutron fields. The various samples were positioned either 22.5 meters directly behind the reactor shadow shield (the location of the payload zone for unmanned SP-100 applications) or they were positioned 3 meters outside the shadow shield in the radial direction. These positions thus represent two extremes for the material activation scenarios.

The amount of induced activity depends on several factors including the cross section for neutron capture as a function of neutron kinetic energy, the abundance of various isotopes present in a given metal sample, and the flux of neutrons present (Chilton et al. 1984). Fig. 5.1 gives a generic plot of induced fractional activity as a function of time expressed in units of the half-life of the induced species. At an ordinate value of 1.0, the material has been sufficiently irradiated by neutrons so as to reach its saturation activity at which time the production rate of target atoms by radioactivation exactly balances the loss rate due to radioactive decay. The absolute value of the saturation activity depends upon the magnitude of the three factors mentioned above. The time to reach saturation activity is dependent upon the half-lives of the induced species and the irradiation time of the sample. Essentially one-half of the maximum activity is achieved after one product half-life, whereas 99% of the saturation activity is reached only after 6.64 product half-lives. Three irradiation times were considered in this work: a 4-hour neutron irradiation, a 30-day neutron irradiation, and a continuous irradiation for 10-years. The latter essentially ensures that saturation activity is achieved for all sixteen of the metal samples considered.

At this point, a direct comparison of the induced activity does not in and of itself allow for a quantitative comparison of the external radiation hazard of the various activated samples. The decay scheme of each induced species must be considered. Nonpenetrating radiations such as alpha particles and beta particles contribute minimally to external exposures to individuals provided the samples (e.g., tools) are shielded in some type of storage container or locker. Gamma-rays as thus the main component of the decay scheme which would contribute to any external dose. Consequently, external doses were calculated at a distance of one meter from each of the irradiated samples consider above. The analogy would be that a space station crew member would retrieve an activated tool from the co-orbiting platform and subsequent return to the station where he or she would remain in close vicinity to the sample or tool for an extended period. It is on this basis that a relative comparison of the various metal constituents can be compared.

Activity calculations were made using the activation analysis code REAC2 which considered the changes in composition of materials subjected to neutron irradiation fields (RSIC 1994). The code considers secondary radioactivation of activation products as well as various pathways of radioactivation such as (n,2n), (n,p), and (n,α) capture reactions in addition to radiative capture reactions of the type (n,γ).

RESULTS AND DISCUSSION

The dosimetry results for the irradiation of both a 125 cm^3 sample of metal and a 1-gram sample of metal 22.5 meters behind the shadow shield of an operating SP-100 reactor are shown in Figs. 5.2 and Figs. 5.3, respectively. The ordinate of both figures demonstrates that the radiological concern is minimal for metallic objects or tools irradiated within neutron flux of an operating SP-100 reactor within the confines of the reactor shadow shield. As a general trend, the data demonstrate that increasing neutron irradiation will result in a larger radioactivity inventory thus delivering a larger cumulative dose to the crew member at later times. This general trend does have its exception, however, as indicated for the tin samples. In this particular case, the large mixture of activation products [7 radioisotopes of Sn considering only the (n,γ) reactions] coupled with both their gamma-ray spectra, their half-lives, and the contribution of secondary activation pathways, results in a subsequent six-month exposure to the crew which is greater for the 4-hour neutron exposure than in the case of the 30-day neutron exposure.

More definitive conclusions can be drawn by looking at the potential radiological hazards associated with materials exposed to the reactor neutron field outside the shadow shield. Dosimetry results for the irradiation of both the 125 cm^3 and the 1-gram sample of metal positioned 3 meters from the reactor in the radial direction are shown in Figs. 5.4 and 5.5, respectively, for each of the three irradiation times. While the post-irradiation exposure scenario used in this analysis is rather extreme (a one-meter separation for six months), substantial radiation doses might be delivered to crew members retrieving tools or other materials which are exposed to the out-of-shadow neutron fields. Fig. 5.4 indicates that for the 125 cm^3 samples exposed to the out-of-shadow neutron flux for 4-hours, 10 out of the 16 metals (Au, Co, Mg, Mn, Ni, Sn, Ta, W, Zn, Zr) would result in six-month radiation doses exceeding or closely approaching the 0.2 Sv LBAD-lt dose budget. If the neutron exposure is increased to 30-days, essentially all of the 16 metals samples considered would result in cumulative exposures to the crew members exceeding the 0.2 Sv dose-budget limit.

Substantially lower cumulative doses would result if the samples are considered to be of equal mass (1 gram) and not of equal volume (125 cm^3). Fig. 5.5 shows that for a 4-hour neutron exposure out-of-shadow, cumulative exposures to the crew are

substantially below the 0.2 Sv dose-budget limit. The exceptions are gold and tantalum which would deliver doses of 0.029 Sv (2.9 rem) and 0.012 Sv (1.2 rem), respectively. If the neutron irradiation is extended to 30 days, one-gram samples of gold, cobalt, and tantalum would result in exposures exceeding the dose budget. Additional metals of concern would be nickel, tungsten, and zirconium which would deliver six-month cumulative doses to crew members of 0.049, 0.013, and 0.012 Sv, respectively. Finally, elements such as Cu, Fe, Mg, Mn, and Zn might also pose additional hazards if present in tools and/or material subject to multiyear neutron exposures followed by close contact with space station crew members.

CONCLUSIONS

A series of simplified activation scenarios were constructed to simulate the possible radioactivation of various metals as might be found in EVA tools which were left in the vicinity of operating SP-100 reactors in LEO. The scenarios are somewhat arbitrary in that the irradiated sample (either 125 cm^3 or 1 gram of pure metal) was assumed to be brought back to the space station and positioned only 1 meter away from a crew member for a period of six-months. Consequently, the scenarios are very conservative and are only intended to give a relative ranking of various metals according to their potential for radiation safety concerns. Even with these provisos, it appears that radioactivation of materials some 20 meters from the reactor in the shadow of the reactor shield complex is of negligible radiological concern. The analysis shows, however, that rather substantial radiological concerns may arise for some elements exposed to the unshielded neutron flux of the operating reactor in the radial direction. Elements of potential concern in this latter scenario include Au, Co, Ni, Ta, and possibly W and Zr.. For very long irradiations (several years), additional metals of concern would include Cu, Fe, Mg, Mn, and Zn.

References

Chilton, A. B., J. K. Shultis, and R. E. Faw, "Principles of Radiation Shielding", Prentice Hall, Englewood Cliffs, NJ (1984).

Radiation Information Shielding Center, Oak Ridge National Laboratory, REAC2: A Computer Code for Activation and Transmutation of Alloys in NFE Facilities, RISC Computer Code Collection CCC-443, Oak Ridge, Tennessee, January 1994.

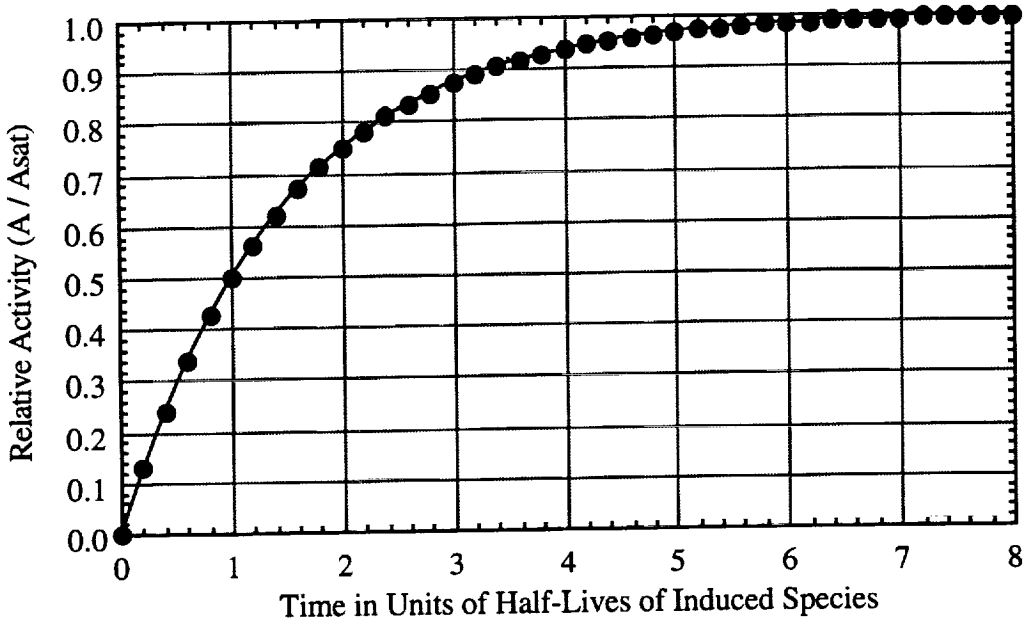

Figure 5.1. Relative fraction of induced saturation activity for an activated radioisotope as a function of the number of half-lives of the induced species.

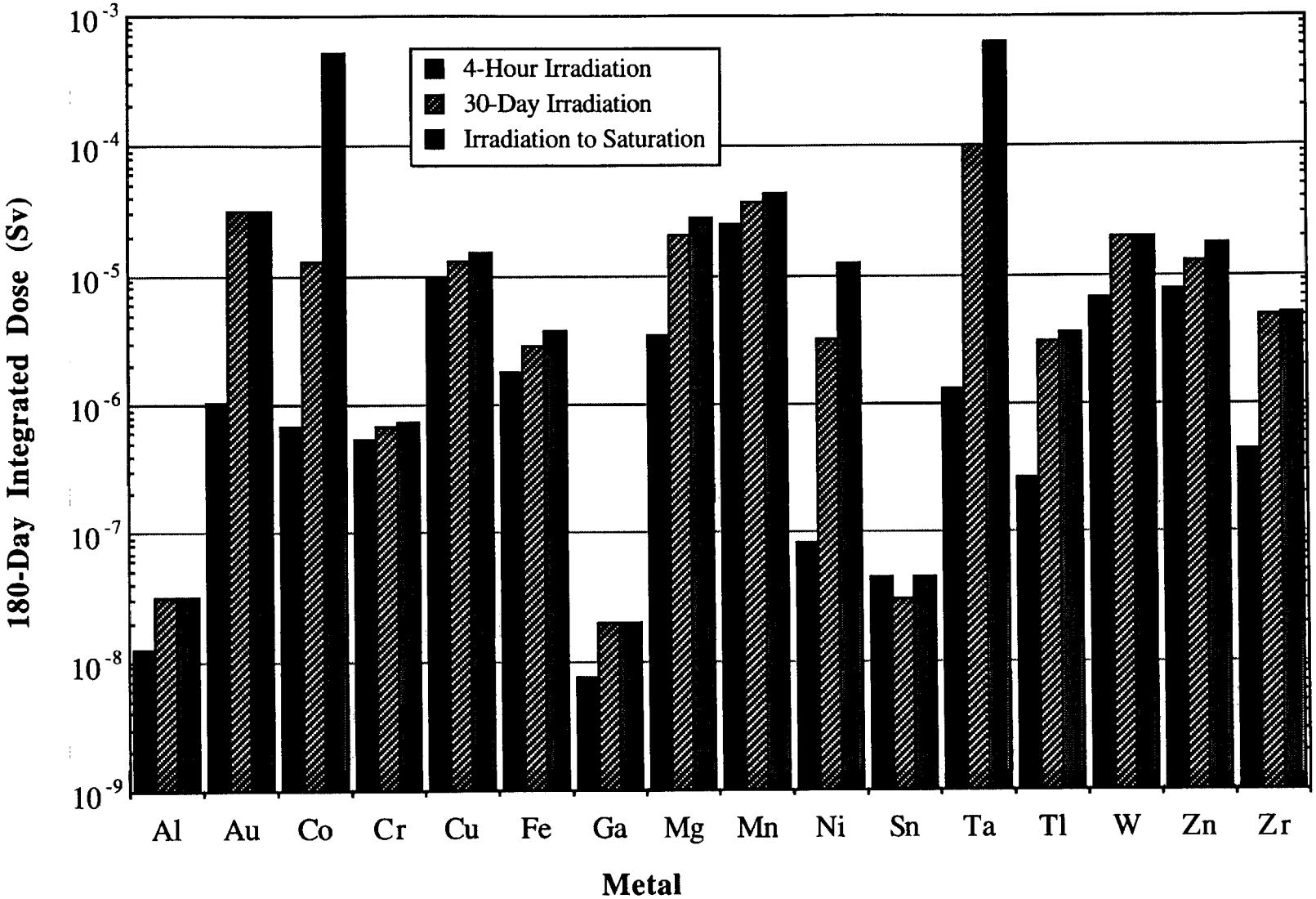

Figure 5.2. Cumulative six-month dose to a hypothetical crew member positioned 1 m from various 125-cm^3 activated metallic samples. The samples were previously exposed to the neutron field 22.5 meters behind the shadow shield of an operating SP-100 reactor. Neutron irradiation times are 4 hours, 30 days, or 10 years as indicated.

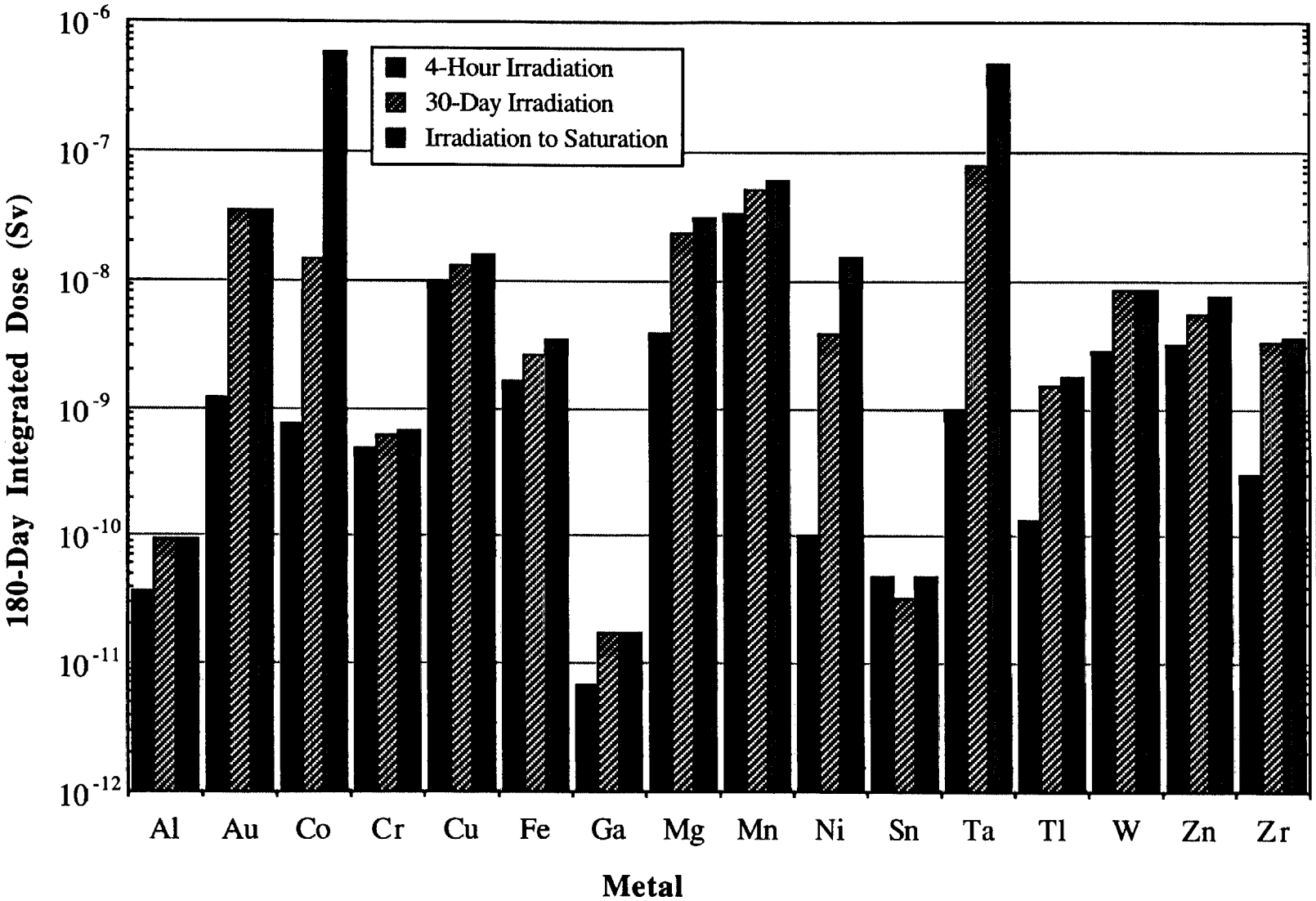

Figure 5.3. Cumulative six-month dose to a hypothetical crew member positioned 1 m from various 1-gram activated metallic samples. The samples were previously exposed to the neutron field 22.5 meters behind the shadow shield of an operating SP-100 reactor. Neutron irradiation times are 4 hours, 30 days, or 10 years as indicated.

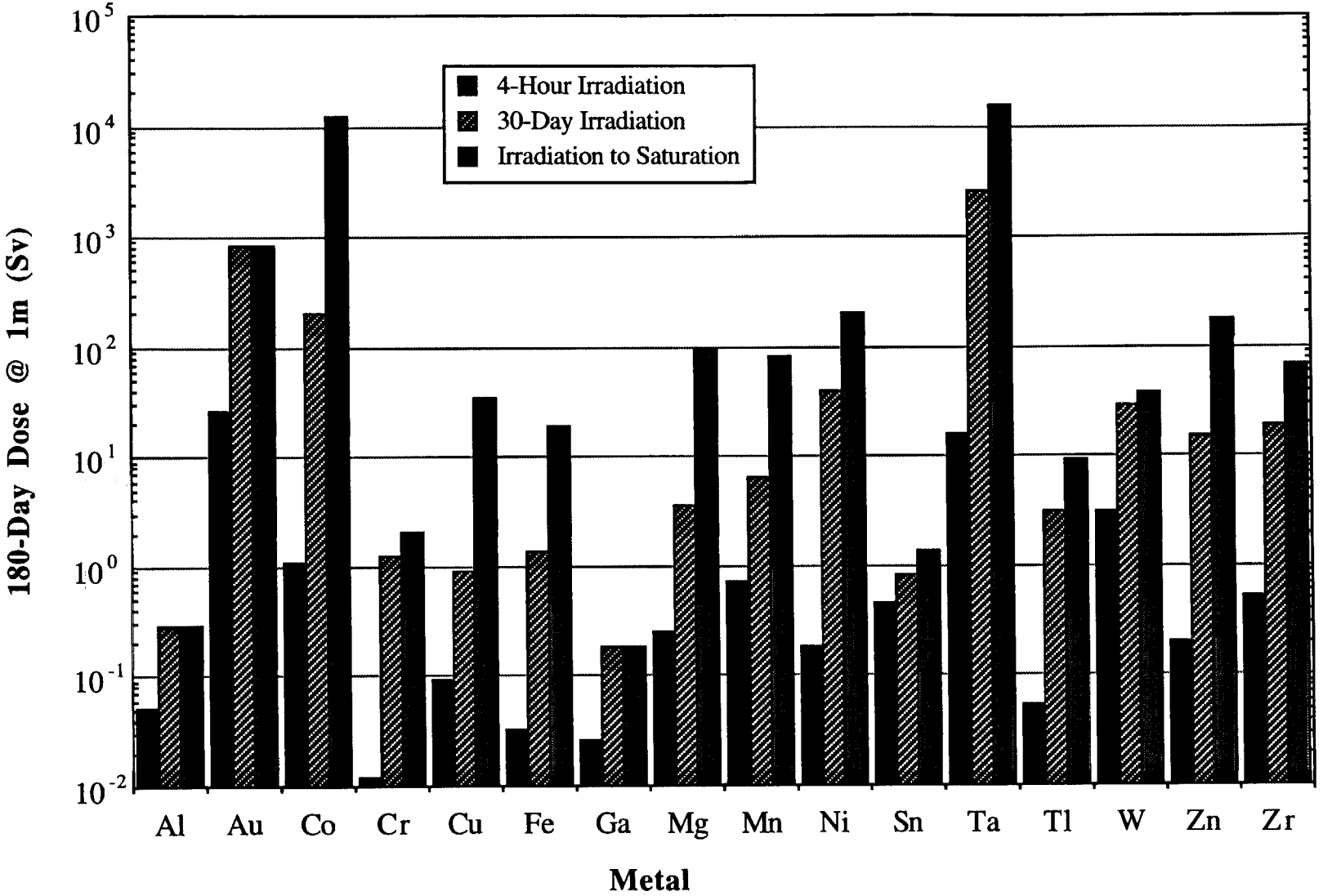

Figure 5.4. Cumulative six-month dose to a hypothetical crew member positioned 1 m from various 125-cm^3 activated metallic samples. The samples were previously exposed to the neutron field 3 meters outside the shadow shield of an operating SP-100 reactor. Neutron irradiation times are 4 hours, 30 days, or 10 years as indicated.

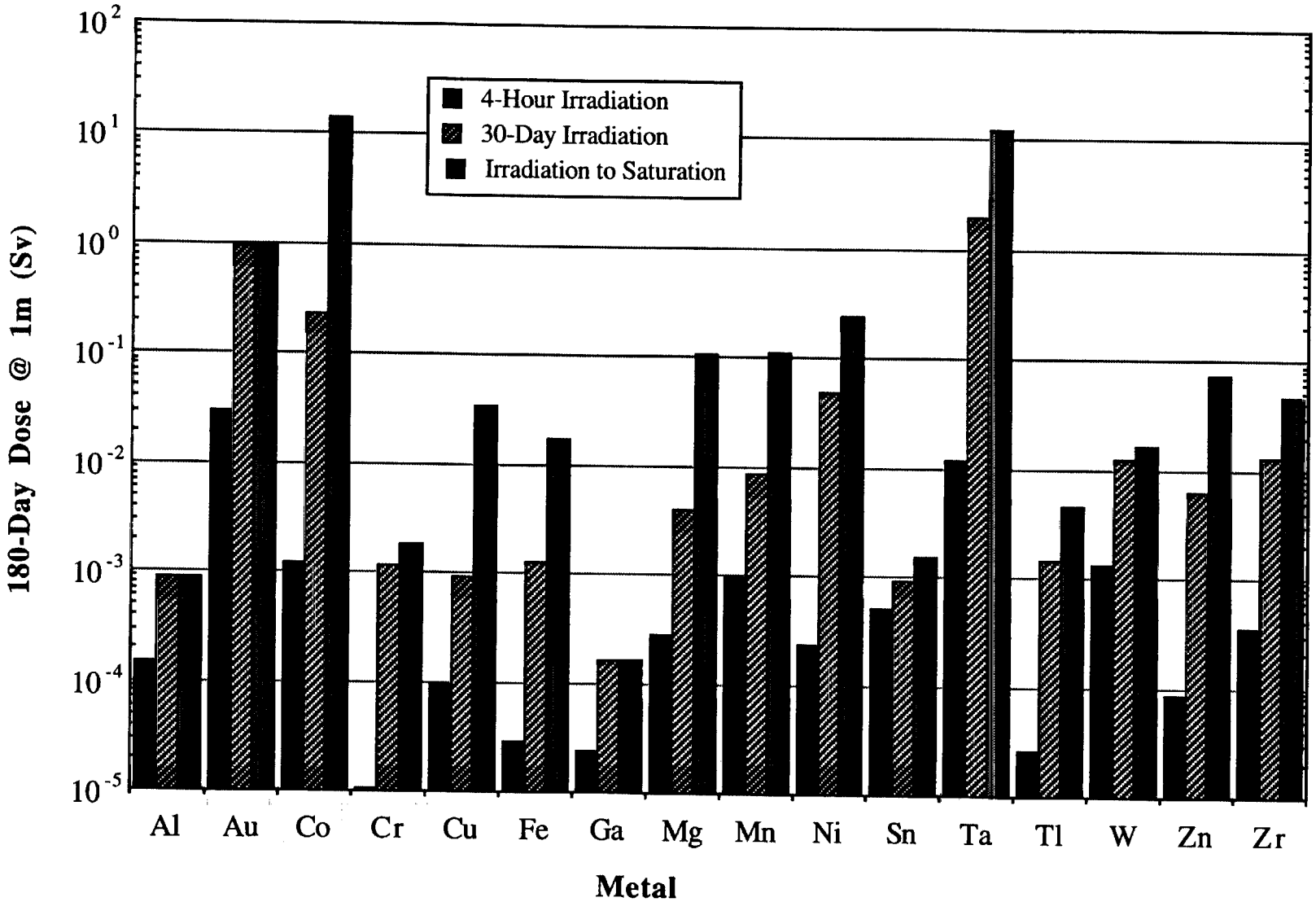

Figure 5.5. Cumulative six-month dose to a hypothetical crew member positioned 1 m from various 1-gram activated metallic samples. The samples were previously exposed to the neutron field 3 meters outside the shadow shield of an operating SP-100 reactor. Neutron irradiation times are 4 hours, 30 days, or 10 years as indicated.

APPENDIX A

SUMMARY OF RADIATION DOSIMETRY QUANTITIES AND UNITS

INTRODUCTION

This appendix briefly defines the two quantities used in radiation dosimetry: the absorbed dose (D) and the dose equivalent (H). The two are related by the expression $H = \overline{Q}D$, where $\overline{Q}$ is a dimensionless weighting factor. In this report, the general term radiation "dose" will be used to specify values of dose equivalent.

ABSORBED DOSE

The primary physical quantity used in radiation dosimetry is the absorbed dose (D) and is defined as the net amount of energy deposited per unit mass of tissue or other material. Its traditional unit is the rad which is equal to 100 ergs of energy deposited per gram of material. The S.I. unit of absorbed dose is the gray (Gy) which is equal to one joule deposited per kilogram of material. Consequently, one Gy is equal to 100 rad. Absorbed dose can be measured with devices such as thermoluminescent dosimeters (TLD) or gas ionization chambers. Absorbed doses to internal organs is usually inferred from radiation transport calculations using mathematical phantoms (see Appendix B).

DOSE EQUIVALENT

Not all types of radiation produce the same amount of biological damage per unit absorbed dose. In particular, charged particles with high rates of energy loss per unit track length, such as neutron recoils and low-energy protons, are more effective in producing biological effects than those with lower rates of energy loss, such as electrons and high-energy protons. This rate of energy loss is defined as the LET, or linear energy transfer, of the particle.

To account for the greater biological effectiveness of high-LET radiations, the quantity dose equivalent (H) is defined for use in radiation protection:

$$H = \overline{Q}D ,$$

where D is the absorbed dose and $\overline{Q}$ is a dimensionless weighting parameter called the average quality factor. The traditional unit of dose equivalent is the rem and is equal to Q times the absorbed dose in rad. The S.I. unit of dose equivalent is the sievert (Sv) and is equal to Q times the absorved dose in Gy. Consequently, a dose equivalent of one Sv is equal to 100 rem.

For a given radiation field and a point of interest within the body, the average quality factor can be determined either by detailed measurement or by radiation transport calculations using the expression:

$$\overline{Q} = \frac{1}{D}\int_{L_{min}}^{L_{max}} Q_L \, D_L \, dL \, ,$$

where D is the total absorbed dose, D_L is the absorbed dose delivered by particles in the LET range L to L+dL, and Q_L is the quality factor as a function of LET as shown in Figure A.1. Note that for low-LET radiations (LET < 3.5 keV/μm), Q is always equal to one. For very high-LET radiations (LET > 175 keV/μm), Q is always equal to its maximum value of 20.

In many situations, only the type of radiation present and the total absorbed dose are known; consequently, single values of $\overline{Q}$ may be used as shown in Table A.1. Recently, however, several radiation protection organizations have issued reports recommending that $\overline{Q}$ for fast neutrons be increased from 10 to 20 (ICRP 1985, NCRP 1987) or 25 (ICRU 1986). This increased level of conservatism places a greater emphasis on making actual LET spectral measurements within radiation fields of interest.

References

ICRP (1977) Recommendations of the International Commission on Radiological Protection, ICRP Publication 26, International Commission of Radiological Protection, Pergamon Press, New York, 1977.

ICRP (1985) Statement from the 1985 Paris Meeting of the International Commission on Radiological Protection, ICRP Publication 45, International Commission of Radiological Protection, Pergamon Press, New York, 1985.

ICRU (1986) The Quality Factor in Radiation Protection, Report of the Joint Task Group of the ICRP and the ICRU, ICRU Report 40, International Commission on Radiation Units and Measurements, Bethesda, Maryland, April 1986.

NCRP (1971) Basic Radiation Protection Criteria, NCRP Report No. 39, National Council on Radiation Protection and Measurements, Bethesda, Maryland, January 1971.

NCRP (1987) Recommendations on Limits for Exposure to Ionizing Radiation, NCRP Report No. 91, National Council on Radiation Protection and Measurements, Bethesda, Maryland, June 1987.

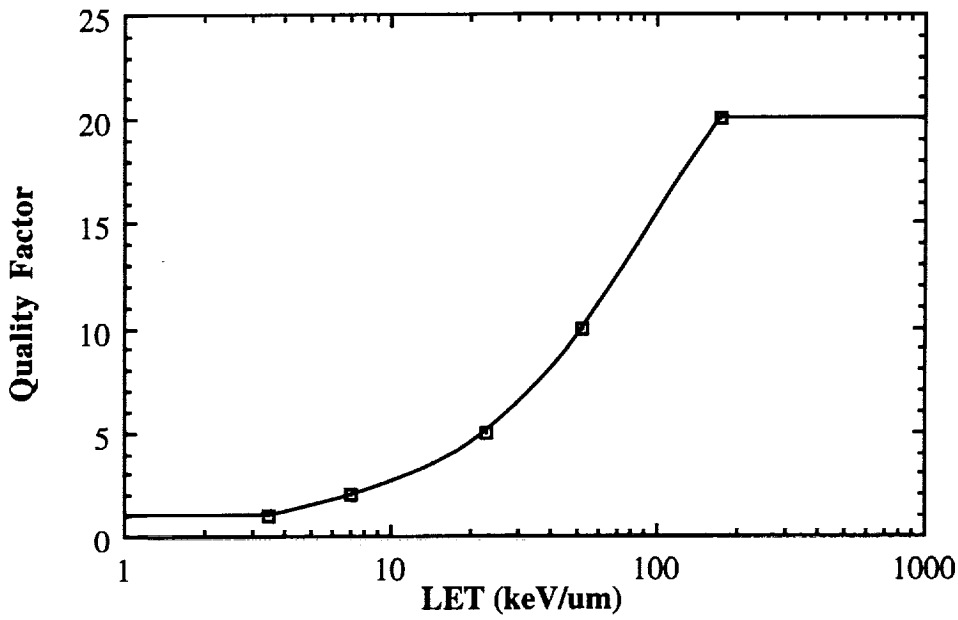

Figure A.1 Quality Factor as a Function of LET (ICRP 1977).

Table A.1 Average Values of Quality Factor for Various Radiations.
[Source: Table 5 of NCRP Report No. 39 (NCRP 1971)]

Radiation Type	Rounded Quality Factor
X-rays, Gammas, Electrons	1
Thermal Neutrons	2
Fast Neutrons	10
Protons	10
Alpha Particles	20
Fission Fragments, Recoil Nuclei	20

APPENDIX B

FLUENCE-TO-ORGAN DOSE CONVERSION FUNCTIONS

INTRODUCTION

This appendix describes the method by which radiation doses to the blood forming organs are calculated for both gamma and neutron irradiations. The term "blood forming organ" is a general term denoting the dose at a depth of 5 cm (NCRP 1989). In this report, BFO doses are specifically calculated for the red bone marrow.

CALCULATION OF ORGAN DOSES

The calculation of doses to the various organs of the body is greatly facilitated by the use of organ dose conversion functions (DCF). These functions give the organ dose delivered per unit radiation fluence as a function of particle energy incident upon the body. Thus, the dose H to a particular organ T from radiation type R is determined as:

$$H_{T,R} = \int_0^{E_{max}} \phi_{R,E} \, (DCF)_{T,R,E} \, dE \, ,$$

where $\phi_{R,E}$ is the total fluence (number of particles incident per unit area) for radiation R differential with respect to particle energy E, and $(DCF)_{T,R,E}$ is the dose conversion function for organ T and radiation R.

The radiation source terms $\phi_{R,E}$ for both operating and shutdown NEP and NTR reactors are presented in Chapter 4. Organ DCFs used in this report were take from Report 43 of the International Commission on Radiation Units and Measurements (ICRU) (ICRU 1988). These functions were generated from Monte Carlo radiation transport calculations using detailed mathematical phantoms of the human body (Kramer 1982). ICRU Report 43 graphically displays gamma and neutron dose conversion functions for 12 organs and five irradiation geometries. The five geometries are (1) a broad parallel beam from front to back; (2) a broad parallel beam from back to front; (3) a broad parallel beam from the side; (4) an isotropic field; and (5) a planar isotropic radiation field. This latter field is analogous to an individual being rotated within a broad parallel beam and is the most appropriate for

estimating radiation doses from man-made sources in space. The DCFs given in Report 43 for gamma irradiation were taken from Williams et. al 1985; those for neutron irradiation were taken from Nagarajan et. al 1981.

SELECTED DCFs FOR GAMMAS AND NEUTRONS

Dose conversion functions are given in ICRU Report 43 in the form of discrete values for 14 gamma energies and 16 neutron energies. These values for the red bone marrow are given in Tables B.1 and B.2 for planar isotropic gamma and neutron radiation fields, respectively. To facilitate the dose calculations in this report, the DCF values for gamma irradiation were fit to a third-order polynomial of the type:

$$\ln(DCF_\gamma) = a + b\ln(E_\gamma) + c[\ln(E_\gamma)]^2 + d[\ln(E_\gamma)]^3$$

where $a = -26.368453$, $b = 0.874235$, $c = -0.0468297$, $d = 0.00497059$,
E_γ is in MeV, and DCF_γ is in Sv cm^2.

This function is shown in Figure B.1 along with the tabulated values of Table B.1. The DCF values for neutron irradiation were fit to a fifth-order polynomial of the type:

$$\ln(DCF_n) = a + b\ln(E_n) + c[\ln(E_n)]^2 + d[\ln(E_n)]^3 + e[\ln(E_n)]^4 + f[\ln(E_n)]^5$$

where $a = -23.243145$, $b = 0.968684$, $c = -0.0472173$, $d = -0.0327160$,
$e = -0.00302264$, $f = -0.0000852384$, E_n is in MeV,
and DCF_n is in Sv cm^2.

This function is displayed in Figure B.2. It is important to note that this functional form is only valid for neutron energies between 1 eV and 15 MeV; functional values below 1 eV are greatly overestimated and those above 15 MeV are greatly underestimated.

References

ICRU (1988) Determination of Dose Equivalents for External Radiation Sources - Part 2, ICRU Report 43, International Commission on Radiation Units and Measurements, Bethesda, Maryland, December 1988.

Kramer, R., M. Zankl, G. Williams, and G. Drexler (1982) The Calculation of Dose from External Photon Exposures using Reference Human Phantoms and Monte Carlo Methods, Part 1. The Male (ADAM) and Female (EVA) Adult Mathematical

Phantoms, GSF-Bericht S-885, Gesellschaft fur Strahlen- und Umweltforschung mbH, Munchen.

Nagarajan, P. S., A. Wittmann, and G. Burger (1981) "Fast Neutron Organ Dose Calculations using a MIRD Phantom," pp. 49-61 in Proceedings of the Fourth Symposium on Neutron Dosimetry, Vol. I, Radiation Protection Aspects, G. Burger and H. G. Ebert, Eds., Commission of the European Communities, Luxembourg.

NCRP (1989) Guidance on Radiation Received in Space Activities, NCRP Report No. 98, National Council on Radiation Protection and Measurements, Bethesda, Maryland, July 1989.

Williams, G., M. Zankl, H. Eckerl, and G. Drexler (1985) The Calculation of Dose from External Photon Exposures using Reference Human Phantoms and Monte-Carlo Methods. Part 2: The Organ Doses from Occupational Exposures, GSF-Bericht S-1079, Gesellschaft fur Strahlen- und Umweltforschung mbH, Munchen.

Table B.1 Gamma Dose to the Red Bone Marrow per Unit Fluence within a Planar Isotropic Radiation Field.
[Source: Fig. B.6 of ICRU Report 43 (ICRU 1988)]

Gamma Energy (Mev)	Dose per Unit Fluence (Sv cm^2)
2.50E-02	5.50E-14
5.00E-02	1.60E-13
6.00E-02	2.00E-13
7.00E-02	2.30E-13
8.00E-02	2.60E-13
1.00E-01	3.30E-13
1.50E-01	5.20E-13
2.00E-01	7.00E-13
3.00E-01	1.20E-12
5.00E-01	1.90E-12
1.00E+00	3.70E-12
3.00E+00	8.50E-12
6.00E+00	1.50E-11
1.00E+01	2.20E-11

Table B.2 Neutron Dose to the Red Bone Marrow per Unit Fluence within a Planar Isotropic Radiation Field.
[Source: Fig. B.33 of ICRU Report 43 (ICRU 1988)]

Neutron Energy (Mev)	Dose per Unit Fluence (Sv cm^2)
1.00E-06	2.90E-12
1.00E-05	2.70E-12
1.00E-04	2.50E-12
1.00E-03	2.40E-12
1.00E-02	2.70E-12
2.50E-02	3.40E-12
5.00E-02	5.50E-12
1.00E-01	1.00E-11
2.80E-01	2.50E-11
5.50E-01	5.20E-11
1.00E+00	9.00E-11
2.50E+00	1.70E-10
5.00E+00	2.50E-10
8.00E+00	3.10E-10
1.20E+01	3.70E-10
1.50E+01	4.00E-10

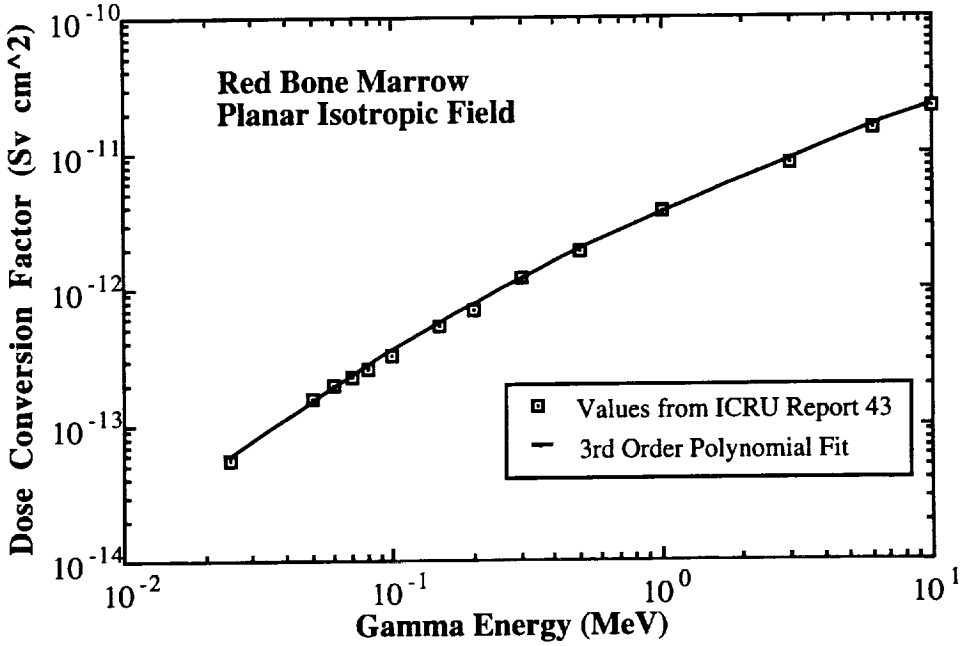

Figure B.1 Dose Equivalent (Sv) to the Red Bone Marrow, per Unit Fluence (cm^{-2}), as a Function of Photon Energy for a Planar Isotropic Radiation Field.

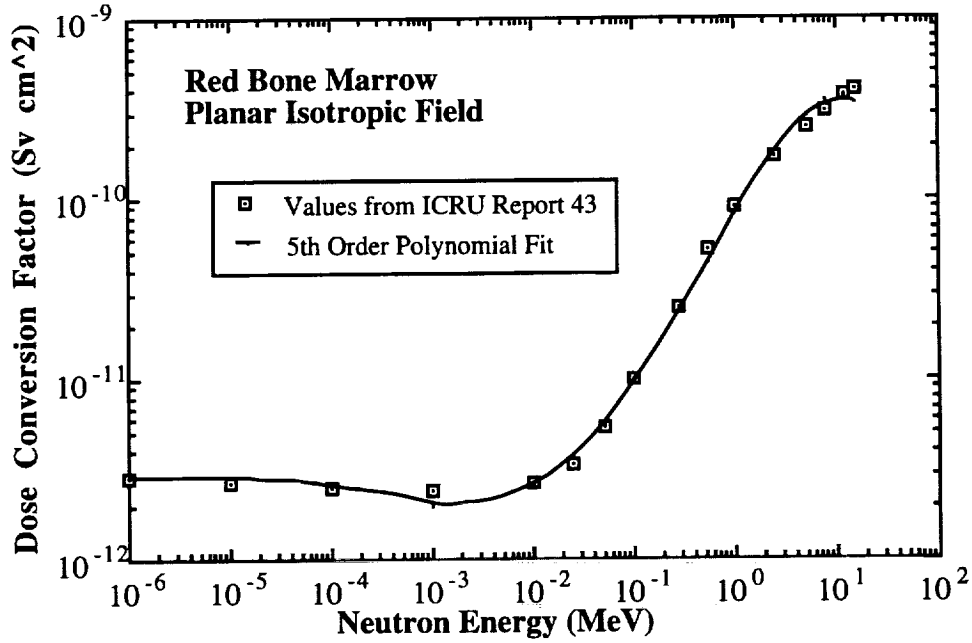

Figure B.2 Dose Equivalent (Sv) to the Red Bone Marrow, per Unit Fluence (cm^{-2}), as a Function of Neutron Energy for a Planar Isotropic Radiation Field.

APPENDIX C

DECAY HEAT CALCULATIONS FOR NUCLEAR REACTORS

INTRODUCTION

This appendix is intended to present the range of decay heat models available in the literature and discuss their advantages and disadvantages. A secondary purpose is to explain the rationale for selecting the particular model employed in this work. In addition, the expressions necessary to implement this model for the cases analyzed (i.e. the NTR and NEP reactors) are developed.

DECAY HEAT MODELS

Immediately after reactor shutdown, the reactor power level is controlled by delayed neutron emission. The power during this period may be described by the simple exponential form shown below:

$$P_s = P_o \, a \, e^{-bt}$$

where 'a' (unitless) and 'b' (time^{-1}) are empirical constants, P_o is the operating reactor power, and P_s is the power of the shutdown reactor. For a typical power reactor, 'a' and 'b' may be taken to be approximately 0.15 and 0.1 sec^{-1}, respectively (Tong and Weisman 1979, Weisman 1977). Since this behavior is only exhibited immediately after reactor shutdown, its contribution was not included in the analyses reported here.

After a few hours following reactor shutdown the reactor power is controlled by decay heat, which is primarily due to the radioactive decay of fission products. Gammas emitted from neutron capture products represent a secondary source of decay heat. The chief neutron capture products of concern for terrestrial reactors are uranium-239 (U-239) and neptunium-239 (Np-239), which result from neutron capture in U-238. This will not be of importance for most space reactor designs since their fuels are typically highly enriched in U-235 and thus contain only a small amount of U-238. Reactor structural and control materials, which are considered to be of only minor importance in terrestrial power

reactors, are usually the primary source of neutron capture products for most space reactors.

A large number of relatively simple empirical models for post-shutdown decay heat and gamma source terms have been developed and reported in the literature. These are discusses briefly in the following paragraphs.

The first class of decay heat models can be illustrated by the relationship shown below (El-Wakil 1971):

$$\frac{P_s}{P_o} = A\, t_s^{-B}\left[1 - \left(1 + \frac{t_o}{t_s}\right)^{-C}\right]$$

where A, B, and C are empirical constants, t_o is the length of time the reactor has been operated, and t_s is the reactor shutdown time. As before, P_o is the operating reactor power and P_s is the power of the shutdown reactor. El-Wakil (1971) gives these constants as 0.095, 0.26, and 0.2, respectively, for time given in seconds. The bracketed term in this expression accounts for the effect of finite reactor operation times; as this time approaches infinity, the bracketed term goes to unity. Similar expressions are also presented in ANL (1963), in this case the decay power due to gamma and beta emission are given separately and the contributions from various gamma energy groups are illustrated. It should be noted that much of the experimental work providing the foundations for these expressions was performed from the late 1940s through early 1960s. These expressions, while their simplicity is attractive, have been reported to be in error by factors greater than 2 for times in excess of a few hours (England et al. 1975).

Recently, a more accurate class of decay heat models has been developed, evaluated, and verified. These models are based on modern experimental data evaluations and employ sums of exponentials to provide a better empirical fit. An example of this type of model is shown below (Chilton et al. 1984):

$$f_k(t_f) = \sum_{j=1}^{N_k} \alpha_{jk}\, e^{-\lambda_{jk} t}$$

where f_k is the energy release rate per fission for gammas (or betas) in energy group k (MeV/fission/sec), t_f is the time since the fission event of interest occurred, and α_{jk} and λ_{jk}

are empirical constants for energy group k. Various number of decay gamma or beta energy groups have been employed by different investigators. LaBauve et al. (1982) report formulating values for 22, 11, and 6 groups; both LaBauve et al. (1982) and ANS/ANSI (1979) give coefficient sets for a single energy group correlation. N_k is simply the number of terms used to construct the fit. LaBauve et al. (1982) employ 11 terms in their single energy group models and between 9 to 15 coefficients for their 6 energy group expressions; the ANS/ANSI (1979) model makes use of 23 terms in their single energy group model.

In the case where all contributions are lumped into a single energy group, the expression given above reduces to:

$$f(t_f) = \sum_{j=1}^{N} \alpha_j e^{-\lambda_j t}$$

Integrating with respect to both reactor operating and shutdown time yields the gamma energy release rate at the shutdown time of interest. This is discussed in more detail in the following section.

Lastly, it should be noted that a number of detailed computer codes have been developed which are capable of yielding decay heat source terms. The ORIGEN code (Croff 1973), which has been upgraded to the ORIGEN2 version (Croff 1980, Croff 1983 and RSIC 1987), is the best known and most widely utilized. The ORIGEN code series has been extensively verified and is considered a standard for this type of calculation. The CINDER code series (England et al. 1976) can also be used for this purpose. Schenter et al. (1977) provide a discussion and comparison of many of these codes; LaBauve et al. (1982) provide a short listing as well. The main advantage to employing these codes is accuracy. The simple empirical expressions given above were developed using data from terrestrial power reactors and thus will not be as accurate when applied to space reactors which employ different materials and operating conditions. Another advantage to this type of code is that neutron capture and activation effects are explicitly accounted for in the code predictions, although empirical correction factors to account for these phenomena have been developed.

SELECTION AND IMPLEMENTATION OF A DECAY HEAT MODEL

As discussed above, isotope generation and depletion codes such as ORIGEN2 yield the most accurate estimate of the decay gamma and heat source terms. However, to implement these codes requires a good knowledge of the reactor material composition and neutron flux. Since these were not readily available and the project was subject to time constraints, it was judged acceptable to employ one of the empirical exponential summation decay heat models. As noted above, the very simple decay models are not sufficiently accurate for this work. Only the decay gamma source was of interest since the betas will be absorbed within the reactor and the corresponding bremsstrahlung contribution is small compared to the decay gamma source strength.

As discussed in the section above, the gamma energy release rate per fission (MeV/fission/sec) can be expressed as:

$$f(t_f) = \sum_{j=1}^{N} \alpha_j e^{-\lambda_j t}$$

where, as before, t_f is the time since the fission event occurred, and α_j and λ_j are empirical constants. Multiplying this expression by the operating fission rate yields the total shutdown gamma energy release rate; the operating fission rate can be expressed as the reactor power divided by the recoverable energy per fission. The gamma energy release rate per unit time of reactor operation, $F(t_f)$ (in MeV/sec^2), can then be written as:

$$F(t_f) = \left(\frac{P_o}{E_r}\right) \sum_{j=1}^{N} \alpha_j e^{-\lambda_j t}$$

where P_o is the operating power in MeV/s and E_r is the recoverable energy per fission event in MeV/fission. Assuming a constant reactor power, this expression may be integrated with respect to operating time, t_o, to yield the total gamma energy release rate, or power, at some shutdown time, t_s, as shown below:

$$P_{\gamma_s}(t_s) = \left(\frac{P_o}{E_r}\right) \sum_{j=1}^{N} \alpha_j \int_{t_s}^{t_o + t_s} e^{-\lambda_j t_f} \, dt_f = \left(\frac{P_o}{E_r}\right) \sum_{j=1}^{N} \frac{\alpha_j}{\lambda_j} \left(1 - e^{-\lambda_j t_o}\right) e^{-\lambda_j t_s}$$

There are alternate periods of full and reduced power operation in the Mars mission scenarios employed in this work; each period of operation (mission phase) is treated separately and the source terms are summed to compute a total source. Denoting the operating power, operating time, and corresponding shutdown time (i.e. time since that mission phase ended) for each phase with the subscript 'm' and summing over all mission phases yields the total gamma power after reactor shutdown:

$$P_{\gamma_s}(t_s) = \sum_{m=1}^{M} \left[\left(\frac{P_{o_m}}{E_r} \right) \sum_{j=1}^{N} \frac{\alpha_j}{\lambda_j} \left(1 - e^{-\lambda_j t_{o_m}}\right) e^{-\lambda_j t_{s_m}} \right]$$

where M is the total number of mission phases. The procedure employed to compute the shutdown gamma dose using this shutdown gamma power expression is discussed in Chapter 6 of this report.

The expression given above can be integrated with respect to exposure time, t_e, to compute the total gamma energy released during a given exposure period:

$$E_\gamma(t_s, t_{exp}) = \sum_{m=1}^{M} \left[\left(\frac{P_{o_m}}{E_r} \right) \sum_{j=1}^{N} \frac{\alpha_j}{\lambda_j^2} \left(1 - e^{-\lambda_j t_{o_m}}\right) e^{-\lambda_j t_{s_m}} \left(1 - e^{-\lambda_j t_e}\right) \right]$$

As discussed in the preceding section, there are multiple coefficient sets (α_j, λ_j) available that could be employed with the expressions developed above. For the purposes of this work, the single-energy group reported by LaBauve et al. (1982) and given in Table C.1 was employed.

References

ANL (1963) Reactor Physics Constants, ANL-5800, 2nd edition, Argonne National Laboratory, Argonne, IL, pp. 634-7.

ANS/ANSI (1979) American National Standard for Decay Heat in Light Water Reactors, ANSI/ANS 5.1, American National Standards Institute, American Nuclear Society, La Grange Park, IL.

Chilton, A.B, J.K. Shultis and R.E. Faw (1984) Principles of Radiation Shielding, Prentice-Hall, Inc., Englewood Cliffs, NJ, pp. 468-77.

Croff, A.G. (1973) ORIGEN - The ORNL Isotope Generation and Depletion Code, ORNL-4628, Oak Ridge National Laboratory, Oak Ridge, TN.

Croff, A.G. (1980) ORIGEN2 - A Revised and Updated Version of the ORNL Isotope Generation and Depletion Code, ORNL-5621, Oak Ridge National Laboratory, Oak Ridge, TN.

Croff, A.G. (1983) "ORIGEN2: A Versatile Computer Code for Calculating the Nuclide Compositions and Characteristics of Nuclear Materials," Nucl.Tech., 62: 335-52.

El-Wakil, M.M. (1971) Nuclear Heat Transport, International Textbook Co., Scranton, OH, pp. 94-8.

England, T.R., R.E. Schenter and N.L. Whittemore (1976) Gamma and Beta Decay Power Following U-235 and Pu-239 Fission Bursts, LA-6021-MS, Los Alamos National Laboratory, Los Alamos, NM, July 1975.

England, T.R., M.G. Stamatelatos and N.L. Whittemore (1976) "Decay Heating, Gas Content, and Spectra Calculations for Fission Products," in Applied Nuclear Data Research and Development, January 1 - March 31, 1976, LA-6472-PR, Los Alamos National Laboratory, Los Alamos, NM, August 1976, pp. 60-63.

Keepin, G.R. (1965) Physics of Nuclear Kinetics, Addison-Wesley Publishing Co., Reading, MA, pp. 130-42.

LaBauve, R.J., T.R. England, D.C. George and C.W. Maynard (1982) "Fission Product Analytic Impulse Source Functions," Nucl.Tech., 56: 322-39.

RSIC (1987) RSIC Computer Code Collection, ORIGEN2: Isotope Generation and Depletion Code - Matrix Exponential Method, CCC-371, Radiation Shielding Information Center, Oak Ridge National Laboratory, Oak Ridge, TN, Nov. 1987.

Schenter, R.E., F. Schmittroth and T.R. England (1977) "Integral Determination of Fission Product Inventory Decay Power," Review Paper No. 15, Fission Product Nuclear Data IAEA-213, Volume 2, presented at the 2nd IAEA Advisory Group Meeting, held in Petten, Netherlands, 5-9 September 1977.

Tong, L.S. and J. Weisman (1979) Thermal Analysis of Pressurized Water Reactors, 2nd edition, American Nuclear Society, La Grange Park, IL, pp. 50-4.

Weisman, J. (1977) Elements of Nuclear Reactor Design, Elsevier Scientific Publ. Co., Amsterdam, pp. 172-4.

Table C.1 Empirical Constant Set Employed for Gamma Source Term.

Coefficient Index (j)	Alpha (unitless)	Lamda (1/sec)
1	2.808E-11	7.332E-10
2	6.038E-10	4.335E-08
3	3.227E-08	1.932E-07
4	4.055E-07	1.658E-06
5	8.439E-06	2.147E-05
6	2.421E-04	2.128E-04
7	1.792E-03	1.915E-03
8	2.810E-02	1.769E-02
9	1.516E-01	1.652E-01
10	4.162E-01	1.266E+00
11	1.053E-01	5.222E+00

APPENDIX D

FORTRAN PROGRAMS FOR CALCULATING PORTABLE SHIELDING REQUIREMENTS AND REDUCTION IN INCIDENT PROTON SPECTRUM

SHIELD.FOR

```
      program shield
      common/gpcoeff/energy(13,2),coeff(5,13,2,2),ac(13,2,2)
      common/operdr/doserate(13,2)
      common/ger/shutime(37),ger(37,2,2)
      common/power/pgo(2)
      common/choice/iveh,nener,ite,ishut,sttd,iorder
c
c  Open GPCOEFF.DAT, OPERDR.DAT, and GAMENER.DAT and read input data
c
      call getcoeff
      call getopdr
      call getger
c
c  Enter the vehicle type...
c
      write(6,10)
10    format(//1x,'Enter the vehicle type:  1-[NEP] or 2-[NTR]: ',$)
      read(5,*)iveh
      if(iveh.eq.1)then
        nener = 4
      else
        nener = 13
      endif
c
c  Define the operating gamma power (MWth)...
c
      pgo(1) = 25.   * 0.065
      pgo(2) = 1575. * 0.065
c
c  Enter the exposure period...
c
      write(6,15)
15    format(//1x,'Enter the exposure period:  1-[4 h] or 2-[6 mo]: ',$)
      read(5,*)ite
c
c   Enter the previous shutdown time...
c
      write(6,20)
20    format(//1x,'Enter the previous shutdown time:'/)
      do 30 i=1,7
        write(6,25)i,shutime(i),i+10,shutime(i+10),i+20,shutime(i+20),
     *             i+30,shutime(i+30)
25      format(1x,4(2x,i2,'-[',f5.1,']'))
30    continue
      do 40 i=8,10
        write(6,35)i,shutime(i),i+10,shutime(i+10),i+20,shutime(i+20)
35      format(1x,4(2x,i2,'-[',f5.1,']'))
40    continue
      write(6,50)
50    format(/1x,'Shutdown Time (days): ',$)
```

```
      read(5,*)ishut
c
c  Enter the source-to-target distance in meters
c
      write(6,55)
55    format(//1x,'Enter the source-to-target distance in (m): ',$)
      read(5,*)sttd
c
c  Determine the Lamination Order
c
      write(6,60)
60    format(//1x,'Enter the lamination order 1-[Al,W] or 2-[W,Al]: ',$)
      read(5,*)iorder
c
c  Enter the Reference Dose Limit
c
      write(6,70)
70    format(//1x,'Enter the desired dose limit (Sv): ',$)
      read(5,*)refdose
c
c  Enter the maximum tungsten shield thickness
c
      write(6,80)
80    format(//1x,'Enter the max. W shield thickness (g/cm2): ',$)
      read(5,*)rxwmax
c
c  Perform the dose calculations...
c
      write(6,90)refdose
90    format(//1x,'Shield Thicknesses for Reference Dose (Sv): ',f5.2/
     *         1x,'W(g/cm2)    Al(g/cm2)'/)
      rxw = 0.0
100   rxa = 0.0
      rxal = 0.0
110   call dosecalc(rxa,rxw,dose)
      if (dose.gt.refdose) then
        rxal = rxa
        rxa = rxa + 5.
        go to 110
      else
        rxah = rxa
        iter = 1
        go to 120
      endif
120   rxa = (rxal + rxah)/2.
      call dosecalc(rxa,rxw,dose)
      if (abs((dose - refdose)/refdose).lt.0.001) then
        write(6,125)rxw,rxa
125     format(2x,f7.2,5x,f7.2)
        goto 130
      elseif (dose.gt.refdose) then
        rxal = rxa
      else
        rxah = rxa
      endif
      iter = iter + 1
      if (iter.gt.1000) stop
      go to 120
```

```
130    rxw = rxw + 5.
       if (rxw.gt.rxwmax) then
         stop
       else
         goto 100
       endif
       end

       block data
       common/gpcoeff/energy(13,2),coeff(5,13,2,2),ac(13,2,2)
       common/operdr/doserate(13,2)
       data energy/26*0.0/,coeff/260*0.0/,ac/52*0.0/
       data doserate/26*0.0/
       end


       subroutine dosecalc(rxa,rxw,dose)
       common/gpcoeff/energy(13,2),coeff(5,13,2,2),ac(13,2,2)
       common/operdr/doserate(13,2)
       common/ger/shutime(37),ger(37,2,2)
       common/power/pgo(2)
       common/choice/iveh,nener,ite,ishut,sttd,iorder
       doseaw = 0.0
       dosewa = 0.0
       do 100 ie = 1,nener
c
c  Determine the Unshielded Gamma Dose
c
         usdr = doserate(ie,iveh) * ger(ishut,ite,iveh) / pgo(iveh)
         usdr = usdr / (sttd**2)
c
c  Determine the Reduction in Uncollided Photon Flux
c
         aca = ac(ie,1,iveh)
         acw = ac(ie,2,iveh)
         rmuxa = aca * rxa
         rmuxw = acw * rxw
         rmux = rmuxa + rmuxw
         expterm = exp(-rmux)
c
c  Determine Buildup Factors
c
         aa  = coeff(1,ie,1,iveh)
         ba  = coeff(2,ie,1,iveh)
         ca  = coeff(3,ie,1,iveh)
         da  = coeff(4,ie,1,iveh)
         xka = coeff(5,ie,1,iveh)
         aw  = coeff(1,ie,2,iveh)
         bw  = coeff(2,ie,2,iveh)
         cw  = coeff(3,ie,2,iveh)
         dw  = coeff(4,ie,2,iveh)
         xkw = coeff(5,ie,2,iveh)
         if(rmuxw.gt.0.0)then
           bufaw = bf(rmux,aw,bw,cw,dw,xkw)
         else
           bufaw = bf(rmux,aa,ba,ca,da,xka)
         endif
         bufwa = bf(rmuxw,aw,bw,cw,dw,xkw)*bf(rmuxa,aa,ba,ca,da,xka)
```

```
c
c   Calculate the dose due to gamma energy ie...
c
        doseaw = doseaw + bufaw * expterm * usdr
        dosewa = dosewa + bufwa * expterm * usdr
100   continue
      if (iorder.eq.1) then
        dose = doseaw
      else
        dose = dosewa
      endif
      return
      end


      subroutine getcoeff
      common/gpcoeff/energy(13,2),coeff(5,13,2,2),ac(13,2,2)
c
c   Definitions...
c     energy(13,2):           13 energies, 2 vehicles (NEP,NTR)
c     coeff(5,13,2,2):  5 coeff, 13 energies, 2 materials (Al,W),
c                       2 vehicles (NEP,NTR)
c     ac(13,2,2):       13 energies, 2 materials (Al,W),
c                       2 vehicles (NEP,NTR)
c
      open(unit=1,file='gpcoeff.dat',status='old')
      do 10 ie=1,4
10      read(1,*)energy(ie,1),ac(ie,1,1),ac(ie,2,1)
      read(1,*)
      do 20 ie=1,4
20      read(1,*)energy(ie,1),coeff(1,ie,1,1),coeff(2,ie,1,1),
     *          coeff(3,ie,1,1),coeff(4,ie,1,1),coeff(5,ie,1,1)
      read(1,*)
      do 30 ie=1,4
30      read(1,*)energy(ie,1),coeff(1,ie,2,1),coeff(2,ie,2,1),
     *          coeff(3,ie,2,1),coeff(4,ie,2,1),coeff(5,ie,2,1)
      read(1,*)
      do 40 ie=1,13
40      read(1,*)energy(ie,2),ac(ie,1,2),ac(ie,2,2)
      read(1,*)
      do 50 ie=1,13
50      read(1,*)energy(ie,2),coeff(1,ie,1,2),coeff(2,ie,1,2),
     *          coeff(3,ie,1,2),coeff(4,ie,1,2),coeff(5,ie,1,2)
      read(1,*)
      do 60 ie=1,13
60      read(1,*)energy(ie,2),coeff(1,ie,2,2),coeff(2,ie,2,2),
     *          coeff(3,ie,2,2),coeff(4,ie,2,2),coeff(5,ie,2,2)
      close(unit=1)
c
c  Verify input by printing Mu/Rho and Buildup Factors for 1 mfp
c  Nuclear Electric Propulsion...
c
c      write(6,70)
c70    format(//1x,'NUCLEAR ELECTRIC PROPULSION (NEP)...'
c     *       //1x,'Energy     MAC-Al       MAC-W        BUF-Al',
c     *          '      BUF-W'//)
c      do 90 ie=1,4
c        acal = ac(ie,1,1)
```

```
c         a  = coeff(1,ie,1,1)
c         b  = coeff(2,ie,1,1)
c         c  = coeff(3,ie,1,1)
c         d  = coeff(4,ie,1,1)
c         xk = coeff(5,ie,1,1)
c         bufal = bf(1.0,a,b,c,d,xk)
c         acw = ac(ie,2,1)
c         a  = coeff(1,ie,2,1)
c         b  = coeff(2,ie,2,1)
c         c  = coeff(3,ie,2,1)
c         d  = coeff(4,ie,2,1)
c         xk = coeff(5,ie,2,1)
c         bufw = bf(1.0,a,b,c,d,xk)
c         write(6,80)energy(ie,1),acal,acw,bufal,bufw
c80       format(1x,f6.3,2x,e11.4,2x,e11.4,2x,e10.3,2x,e10.3)
c90     continue
c
c  Nuclear Thermal Rocket...
c
c       write(6,100)
c100    format(//1x,'NUCLEAR THERMAL ROCKET (NTR)...'
c      *       //1x,'Energy     MAC-Al       MAC-W        BUF-Al',
c      *            '      BUF-W'//)
c       do 110 ie=1,13
c         acal = ac(ie,1,2)
c         a  = coeff(1,ie,1,2)
c         b  = coeff(2,ie,1,2)
c         c  = coeff(3,ie,1,2)
c         d  = coeff(4,ie,1,2)
c         xk = coeff(5,ie,1,2)
c         bufal = bf(1.0,a,b,c,d,xk)
c         acw = ac(ie,2,2)
c         a  = coeff(1,ie,2,2)
c         b  = coeff(2,ie,2,2)
c         c  = coeff(3,ie,2,2)
c         d  = coeff(4,ie,2,2)
c         xk = coeff(5,ie,2,2)
c         bufw = bf(1.0,a,b,c,d,xk)
c         write(6,80)energy(ie,2),acal,acw,bufal,bufw
c110    continue
       end

       function bf(rmux,a,b,c,d,xk)
       if (rmux.gt.0.0) then
         rk = c*rmux**a + d*(tanh(rmux/xk-2.) - tanh(-2.)) /
      *       (1. - tanh(-2.))
         if (rk.eq.1.0) then
           bf = 1. + (b-1.)*rmux
         else
           bf = 1. + (b-1.)*(rk**rmux - 1.)/(rk - 1.)
         endif
       else
         bf = 1.0
       endif
       end
```

```
      subroutine getopdr
      common/operdr/doserate(13,2)
      open(unit=1,file='operdr.dat',status='old')
      read(1,*)
      read(1,*)
      do 10 ie=1,4
10      read(1,*)ener,doserate(ie,1)
      read(1,*)
      do 20 ie=1,13
20      read(1,*)ener,doserate(ie,2)
      close(unit=1)
      return
      end


      subroutine getger
      common/ger/shutime(37),ger(37,2,2)
c
c   Definitions...
c     ger(37,2,2):      37 shutdown times, 2 exposure times (4h,6mo),
c                       2 vehicles (NEP,NTR)
c
      open(unit=1,file='gamener.dat',status='old')
      read(1,*)
      read(1,*)
      do 10 it=1,37
10      read(1,*)shutime(it),ger(it,1,1),ger(it,2,1),ger(it,1,2),
     *           ger(it,2,2)
      close(unit=1)
      return
      end
```

PROTON.FOR

```
      program proton
      common/flux/ebar(25),de(25),protflux(25)
      common/ranges/er(19),ra(19),rw(19),rt(19)
      common/sort/ne(50,25,2)
      common/bin/nbin,ebin(51)
      common/spectra/epen(100,25,2)
      dimension flux(50,2)
c
c  Read input data
c
      call getflux
      call getrange
      call getbins
c
c  Enter the shield lamination thicknesses
c

      write(6,10)
10    format(//1x,'Enter lamination order: 1-[Al,W], 2-[W,Al]: ',$)
      read(5,*)iorder
      write(6,20)
20    format(1x,'Enter the thickness of Al (g/cm2): ',$)
      read(5,*)rxa
      write(6,30)
30    format(1x,'Enter the thickness of W (g/cm2): ',$)
      read(5,*)rxw
c
c   Start the proton transport
c
      do 1200 iprim = 1,25
        cos0 = 0.0
        do 1000 icos0 = 1,100
c
c   Transport through first lamination
c
100       cos0 = cos0 + 0.01
          if (iorder.eq.1) then
            mat = 1
            rx = rxa
          else
            mat = 2
            rx = rxw
          endif
          rxp = rx / cos0
          energy = ebar(iprim)
          call findr(mat,energy,range)
          resrx = range - rxp
          if (resrx.le.0.0) then
            goto 1000
          else
            call finde(mat,resrx,energy)
          endif
c
c   Transport through second lamination
c
```

```
200         if (iorder.eq.1) then
              mat = 2
              rx = rxw
            else
              mat = 1
              rx = rxa
            endif
            rxp = rx / cos0
            call findr(mat,energy,range)
            resrx = range - rxp
            if (resrx.le.0.0) then
              goto 1000
            else
              call finde(mat,resrx,energy)
              epen(icos0,iprim,1) = energy
            endif
c
c  Transport through the 1.0 g/cm2 Al Shield
c
300         rx = 1.0
            mat = 1
            rxp = rx / cos0
            call findr(mat,energy,range)
            resrx = range - rxp
            if (resrx.le.0.0) then
              goto 1000
            else
              call finde(mat,resrx,energy)
            endif
c
c  Transport through 5.0 g/cm2 of Tissue
c
400         rx = 5.0
            mat = 3
            rxp = rx / cos0
            call findr(mat,energy,range)
            resrx = range - rxp
            if (resrx.le.0.0) then
              goto 1000
            else
              call finde(mat,resrx,energy)
              epen(icos0,iprim,2) = energy
            endif
1000     continue
1200   continue
c
c
c
c       do 2000 iprim=1,25
c         write(6,1300)ebar(iprim)
c1300     format(//1x,'Energy: ',e11.4/)
c         write(6,1400)(epen(icos0,iprim,2),icos0=1,100)
c1400     format(1x,5(e11.4,2x))
c2000   continue
c
c  Sort energies
c
        do 1600 ispec = 1,2
```

```
        do 1500 iprim = 1,25
          do 1400 ie = 1,100
            energy = epen(ie,iprim,ispec)
            do 1300 ibin = 2,nbin+1
              if (energy.gt.ebin(ibin)) then
                goto 1300
              else
                ne(ibin-1,iprim,ispec) = ne(ibin-1,iprim,ispec) + 1
                goto 1400
              endif
1300        continue
1400      continue
1500    continue
1600  continue
c
c  Calculate the penetration spectra
c
      do 3000 ispec = 1,2
        do 2000 ibin = 1,nbin
          flux(ibin,ispec) = 0.0
          do 1900 iprim = 1,25
            flux(ibin,ispec) = flux(ibin,ispec) +
     *      protflux(iprim) * (ne(ibin,iprim,ispec)/100) * de(iprim)
1900      continue
        deltae = ebin(ibin+1) - ebin(ibin)
        flux(ibin,ispec) = flux(ibin,ispec) / deltae
2000    continue
3000  continue
c
c  Print the penetration spectrum for the shield
c
      write(6,3100)
3100  format(//1x,'Energy Spectrum Penetrating the Shield'//
     *         1x,'Energy      Flux'/
     *         1x,'(MeV)       (cm2 Mev day)-1'/)
      do 3300 ibin = 2,nbin
        energy = (ebin(ibin+1) + ebin(ibin)) / 2.
        write(6,3200)energy,flux(ibin,1)
3200    format(1x,f8.3,4x,e11.4)
3300  continue
c
c  Print the penetration spectrum in tissue
c
      write(6,3400)
3400  format(//1x,'Energy Spectrum in Tissue'//
     *         1x,'Energy      Flux'/
     *         1x,'(MeV)       (cm2 Mev day)-1'/)
      do 3600 ibin = 2,nbin
        energy = (ebin(ibin+1) + ebin(ibin)) / 2.
        write(6,3500)energy,flux(ibin,2)
3500    format(1x,f8.3,4x,e11.4)
3600  continue
c
c  End of Program
c
      end
```

```
      block data
      common/sort/ne(44,25,2)
      common/spectra/epen(100,25,2)
      data ne/2200*0.0/
      data epen/5000*0.0/
      end


      subroutine getbins
      common/bin/nbin,ebin(51)
      open(unit=1,file='ebins.dat',status='old')
      read(1,*)nbin
      read(1,*)
      do 10 ie=1,nbin+1
10      read(1,*)ebin(ie)
      close(unit=1)
      return
      end

      subroutine getflux
      common/flux/ebar(25),de(25),protflux(25)
      open(unit=1,file='traproton.dat',status='old')
      read(1,*)
      read(1,*)
      do 10 ie=1,25
        read(1,*)e,f,ebar(ie),de(ie),protflux(ie)
10    continue
      close(unit=1)
      return
      end

      subroutine getrange
      common/ranges/er(19),ra(19),rw(19),rt(19)
      open(unit=1,file='ranges.dat',status='old')
      read(1,*)
      read(1,*)
      do 10 ie=1,19
        read(1,*)er(ie),ra(ie),rw(ie),rt(ie)
10    continue
      close(unit=1)
      return
      end


      subroutine finde(mat,r,e)
      common/ranges/er(19),ra(19),rw(19),rt(19)
      dimension rm(19)
      do 10 i=1,19
        if (mat.eq.1) then
          rm(i) = ra(i)
        elseif (mat.eq.2) then
          rm(i) = rw(i)
        else
          rm(i) = rt(i)
        endif
10    continue
c
      if (r.ge.rm(1)) then
```

```
        goto 20
      else
        e = 0.0
        return
      endif
20    do 30 i=2,19
        if (r.gt.rm(i)) then
          go to 30
        else
          ie = i
          go to 40
        endif
30    continue
40    deltar = (alog(r) - alog(rm(ie-1))) /
     *         (alog(rm(ie)) - alog(rm(ie-1)))
      e = exp(deltar * (alog(er(ie))-alog(er(ie-1))) + alog(er(ie-1)))
      return
      end


      subroutine findr(mat,e,r)
      common/ranges/er(19),ra(19),rw(19),rt(19)
      dimension rm(19)
      do 10 i=1,19
        if (mat.eq.1) then
          rm(i) = ra(i)
        elseif (mat.eq.2) then
          rm(i) = rw(i)
        else
          rm(i) = rt(i)
        endif
10    continue
c
      if (e.ge.er(1)) then
        goto 20
      else
        r = 0.0
        return
      endif
20    do 30 i=2,19
        if (e.gt.er(i)) then
          go to 30
        else
          ie = i
          go to 40
        endif
30    continue
40    deltae = (alog(e) - alog(er(ie-1))) /
     *         (alog(er(ie)) - alog(er(ie-1)))
      r = exp(deltae * (alog(rm(ie))-alog(rm(ie-1))) + alog(rm(ie-1)))
      return
      end
```

REPORT DOCUMENTATION PAGE

Form Approved
OMB No. 0704-0188

1. AGENCY USE ONLY (*Leave blank*)	2. REPORT DATE	3. REPORT TYPE AND DATES COVERED
	December 1994	Final Contractor Report

4. TITLE AND SUBTITLE
Design considerations for a space station radiation shield for protection from both man-made and natural sources

5. FUNDING NUMBERS
WU- 488-10-12

6. AUTHOR(S)
Wesley E. Bolch, K. Lee Peddicord
Harry Felsher, and Simon Smith

7. PERFORMING ORGANIZATION NAME(S) AND ADDRESS(ES)
Department of Nuclear Engineering
Texas A&M University
College Station, Texas 77843

8. PERFORMING ORGANIZATION REPORT NUMBER
E- 8680

9. SPONSORING/MONITORING AGENCY NAMES(S) AND ADDRESS(ES)
National Aeronautics and Space Administration
Lewis Research Center
Cleveland, Ohio 44135-3191

10. SPONSORING/MONITORING AGENCY REPORT NUMBER
NASA CR- 195298

11. SUPPLEMENTARY NOTES
Project Manager: Steven M. Stevenson
Advanced Space Analysis Office
NASA Lewis Research Center

12a. DISTRIBUTION/AVAILABILITY STATEMENT
Unclassified - Unlimited
Subject Category

12b. DISTRIBUTION CODE

13. ABSTRACT (*Maximum 200 words*)
This study was conducted to analyze scenarios involving the use of nuclear-powered vehicles in the vicinity of a manned space station (SS) in low-earth-orbit (LEO), an to quantify their radiological impact to the station crew. In limiting the radiatio dose to crew members, mission planners may (1) shut the reactor down prior to re-entry, (2) position the vehicle at a prescribed parking distance, and (3) deploy a radiation shield about the shutdown reactor. While the first two options were explored in previous report (NASA CR-185185), the current report focuses on the third option in which point-kernel gamma-ray shielding calculations were performed for a variety of shield configurations for both nuclear electric propulsion (NEP) and nuclear thermal rocket (NTR) vehicles. For a returning NTR vehicle, calculations indicate that a 14.9 MT shield would be needed to limit the integrated crew exposure to no more that 0.05 Sv over a period of six months (25% of the allowable exposure to man-made radiation sources). During periods of low vehicular activity in LEO, the shield may be redeployed about the SS habitation module in order to decrease crew exposures to trapped proton radiations by approximately a factor of 10 The corresponding shield mass required for deployment at a returning NEP vehicle is 2.21 MT. Additional scenarios examined include the radioactivation of various metals as might be found in tools used in EVA activities.

14. SUBJECT TERMS
Space Station, Radiation Dose Assessment, NEP and NTR Vehicles, Radiation Shield Design, Neutron Activation

15. NUMBER OF PAGES
81

16. PRICE CODE
A05

17. SECURITY CLASSIFICATION OF REPORT	18. SECURITY CLASSIFICATION OF THIS PAGE	19. SECURITY CLASSIFICATION OF ABSTRACT	20. LIMITATION OF ABSTRAC
Unclassified	Unclassified	Unclassified	